



**HAL**  
open science

## Lithium enrichment processes in sedimentary formation waters

Elza J.M. Dugamin, Michel Cathelineau, Marie-Christine Boiron, Antonin Richard, Frank Despinois

► **To cite this version:**

Elza J.M. Dugamin, Michel Cathelineau, Marie-Christine Boiron, Antonin Richard, Frank Despinois. Lithium enrichment processes in sedimentary formation waters. *Chemical Geology*, 2023, 635, pp.121626. 10.1016/j.chemgeo.2023.121626 . hal-04272518

**HAL Id: hal-04272518**

**<https://hal.univ-lorraine.fr/hal-04272518>**

Submitted on 6 Nov 2023

**HAL** is a multi-disciplinary open access archive for the deposit and dissemination of scientific research documents, whether they are published or not. The documents may come from teaching and research institutions in France or abroad, or from public or private research centers.

L'archive ouverte pluridisciplinaire **HAL**, est destinée au dépôt et à la diffusion de documents scientifiques de niveau recherche, publiés ou non, émanant des établissements d'enseignement et de recherche français ou étrangers, des laboratoires publics ou privés.

## **Lithium enrichment processes in sedimentary formation waters**

Elza J.M. Dugamin<sup>1</sup>, Michel Cathelineau<sup>1\*</sup>, Marie-Christine Boiron<sup>1</sup>, Antonin Richard<sup>1</sup>, Frank Despinois<sup>2</sup>

1 University of Lorraine, CNRS, CREGU, GeoRessources, Nancy, France

2 TotalEnergies, Centre Scientifique et Technique Jean Féger, Pau, France

\*Corresponding author: michel.cathelineau@univ-lorraine.fr

Keywords: Lithium, formation waters, sedimentary basin, evaporite, water-rock interaction

### **Abstract**

Reservoirs exploited for oil, gas, or geothermal energy in sedimentary basins may represent an alternative lithium resource to salars and hard rocks. Similarities in the geochemical characteristics of the basins were searched using a database of 2,400 water analyses available from more than 40 sedimentary basins worldwide, notably a selection of representative geochemical trends on 13 basins. The objective was to understand better the factors controlling Li concentrations and the potentiality of such basins for the Li-recovery. Considering Li-Cl and Mg-Cl relationships, major cation (Na/K, Na/Ca) and halogen (Cl/Br) ratios, Li concentrations are monitored in several basins by mixing processes between low salinity recharge waters, seawater and brines. Lithium concentrations span three orders of magnitude in brines between evaporated seawater that has passed saturation with halite and a particularly Li-enriched pole. In the latter, significant Li-enrichment is obtained when brines are primary, in equilibrium with halite, and then enriched in Li through fluid-rock interaction processes. Li-rich lithologies such as volcanic rocks, Li-enriched clay formations, or Li-phyllsilicates dispersed in siliciclastic rocks or the underlying crystalline basement probably act as the primary Li sources. Finally, Li extraction is promoted by the rise in temperature, which explains the high Li concentrations in the waters of

geothermal systems. Therefore, favourable reservoirs for Li-rich brines are characterised by a brine collection from evaporites during tectonic events, such as compressive events or salt tectonics, at a relatively short distance from the present reservoir. They must be preserved from convection and surface water ingress via recharge zones to prevent dilution and Li depletion.

## 1. Introduction

Lithium is an economically important element in transitioning to low-carbon energy, especially for Li-ion rechargeable batteries (Bibienne et al., 2020, Nate et al., 2021). Most primary lithium resources are currently exploited in pegmatites (Greenbushes, Australia, Yaksic and Tilton, 2009; Mohr et al., 2010; Labbe and Daw, 2012), closed-basin brines (salar), primarily in South America (Salar de Atacama, Chile; Salar de Hombre Muerto and Puna, Argentina; Salar de Uyuni, Bolivia (Lopez Steinmetz et al., 2018, 2020; Lopez Steinmetz and Salvi, 2021) and in Lake Qaidam, China; Ericken and Salas, 1987; Bradley et al., 2017, USGS, 2021). Li-enrichment in closed surficial basins is well-known and has been reviewed by Munk et al., (2016).

Groundwater in sedimentary basins, particularly oilfield brines and saline formation waters, can also contain significant Li concentrations, reaching values above 100 mg.l<sup>-1</sup> (e.g. Smackover Formation (Gulf Coast, USA; Collins, 1975). These metal-rich sedimentary formation waters are considered potential "liquid ores" (Alexeev et al., 2020) and represent a good Li resource that can contribute significantly to meeting growing global demand (Dugamin et al., 2021).

The bulk chemical evolution of formation waters in sedimentary basins, such as the role of water-rock interactions (diagenetic reactions), the location of enhanced flow and the timing of fluid migration, have been studied for decades (e.g. White, 1965, Carpenter et al., 1974; Carpenter, 1978; Collins, 1975; Land and Prezbondowski, 1981; Hanor, 1987; Kharaka et al., 1987; McCaffrey et al., 1987; Morton and Land, 1987; Moldovanyi and Walter, 1992; Land and Macpherson, 1992; Stueber et al., 1993; Land, 1995; Davisson and Criss, 1996; Kharaka and Hanor, 2003; Lowenstein et al., 2003; Boiron et al., 2010). However, Li behaviour is much less documented in these deep reservoirs than in closed surficial basins. The sources and mechanisms of Li enrichment remain debated and poorly understood. Fontes and Matray (1993) and, more recently, Coffey et al. (2021) have provided hypotheses on the origin of Li excess in sedimentary basin formation waters: (1) Li-enrichment through diagenetic reactions, including water uptake and Li gains from the host sediments; (2) increased Li in the water source, for instance, paleo- seawaters which may be significantly different from modern seawater and (3) Li enrichment

through evaporation, the evaporated waters being trapped in evaporites or sediments. Understanding such processes is of great interest for the current prospection of reservoirs such as those from the Rhine graben in France and Germany (Sanjuan et al., 2010, 2022) and for recycling water from oil fields (Kumar et al., 2019).

This paper discusses the distribution of Li concentrations in waters from sedimentary basins and the processes that modify these concentrations (mixing, dilution, nature of the different water end-members). The study is based on a compilation of chemical analyses of present-day formation waters from oil and gas reservoirs for which data are available but still not examined from the point of view of Li enrichment processes. Besides, an inventory of Li concentration ranges in rock-forming minerals and rocks has been set up to document the Li cycle. The ultimate objective was to define the standard features of fluids highly enriched in Li and the main processes controlling such enrichment in sedimentary reservoirs. Finally, we examined if such fluids share similar characteristics with brines from salars.

## **2. Data compilation and processing**

All geochemical and physical data for each sedimentary basin used in this study are derived from a compilation of literature data. A database of water analyses from 40 sedimentary basins worldwide, representing approximately 2,400 individual analyses, was first compiled to analyse the factors controlling Li concentrations (Dugamin 2022, Dugamin et al., submitted). All the selected sedimentary waters correspond to reservoir waters (i.e. "formation waters"). Similarities in the geochemical features of Li-rich brines were defined by comparing the relationships between Li concentrations, major cation (Na, K, Ca, Mg) and halogens (Cl, Br) ratios. These observations let us choose 13 out of the 40 basins, which waters share similar features (Fig. 1), and represent the main geochemical trends worldwide. Table 1 provides the location of the selected basins and the chemical composition of their formation waters (Li, Cl, Mg concentrations, Cl/Br, Na/Ca and Na/K ratios).

Data quality and representativeness from the published sources have been scrutinized. The solute concentration data are reported in various units (e.g. ppm, mg.l-1, mmol.l-1, mol.kg-1, meq.l-1). All data were converted to mg.l-1 before being added to the database. The density used for some conversions was either provided in the published sources or set at 1 g.cm-3 (density of pure water at 25°C at 1 atmosphere) by default. The salinity, taken as total dissolved solids (TDS), was calculated as the sum of the available concentration of major ions ( $\text{Na}^+$ ,  $\text{K}^+$ ,  $\text{Ca}^{2+}$ ,  $\text{Mg}^{2+}$ ,  $\text{Cl}^-$ ,  $\text{SO}_4^{2-}$ ,  $\text{NO}_3^-$ ,  $\text{HCO}_3^-$ ) compiled

from published sources and expressed in mg.l-1. Cl, Na, Ca, K and Mg concentrations in formation waters are reported in more than 90% of published sources, but other anion concentration data are not always available. The database did not include the solute concentrations for suspected contamination in the published sources. The analysis of the electrical balance values and the limits of detection (in particular, the proportion of data above limits of detection) provide a first-order control on data quality.

The reservoirs considered in this compilation were subjected to oil and gas extraction and one for geothermal energy (Salton Trough), as presented in Tables 1 and 2. The stratigraphy data (age of sedimentary basins, description of the lithology, presence of salt beds and diapirs, presence of volcanic and crystalline rocks as potential source rocks) are presented in Table 2. Reservoirs are mostly siliciclastic formations, except those located on both sides of the Mexico Gulf (Gulf Coast, Salinas-Sureste) and Zagros, where limestones are reservoirs. The selected reservoirs are hosted by sedimentary formations covering an extensive range of ages from Late Proterozoic to Cenozoic. The basins share the presence of evaporite layers affected in several basins by diapirism and salt tectonics.

Salars from South America were considered for comparison. The same chemical parameters were thus compiled for 18 closed basins and 4 salt lake waters (Table 3).

In addition, to assess potential sources of Li, a compilation of rocks and minerals and their associated Li concentrations from published sources was carried out (Supplementary table A).

### **3; Geochemical data processing**

The following sections compare the relationships between Li, Cl, halogen ratio (Cl/Br), and major cation (Na, K, Ca and Mg) ratios for the 13 selected sedimentary basins and salars.

#### **3.1 Water types**

The general characteristics of formation waters are shown in the Piper diagram (Fig. 2A), where they are compared to salar waters (Fig. 2B). The prominent feature of the studied waters is the predominance of Na and Cl as most data points plot at the Na + K and Cl + NO<sub>3</sub> end-members. Exceptions are: i) the Delaware waters characterised by a mixing trend between a sulfate Mg-(Ca) rich end-member and the Na-Cl end member, ii) two basins with bicarbonate waters show a Na to Ca-Mg trend typical of waters equilibrated in limestone formations (Zagros, North German for the Mesozoic cover), and iii) the Michigan basin waters with an extended trend from the Na-(Cl) corner to a Ca-Mg-Cl end member. Salar

waters as sedimentary basin waters plot close to the Na+K and Cl+NO<sub>3</sub> corners. Several trends towards a Ca + Mg end member are specific to some salars such as Atacama, Ascota, Loyoques or Alconcha. The four latter also show a more carbonated feature and a wider dispersion than sedimentary basins. A sulfate contribution is found in salt water lakes such as Minique, Miscanti and La Azufrera, as well as in the waters with a significant carbonate content above cited.

The Li-Cl binary plot discriminates four main types of fluid end-members based on Cl and Li concentrations (Fig. 3 and 4): (i) low salinity waters (dilute water noted DW) close to rainwaters or river waters indicated by light blue domains in figure 3, (ii) seawater (noted SW), (iii) evaporated seawater (noted ESW), and (iv) a brine with Cl concentrations close to those of halite saturation, but with exceptionally high Li concentrations (1 to 2 orders of magnitude higher than those of evaporated seawater saturated to halite (Li-rich brine, noted LiRB). Plotting all Li versus Cl data reveals four types of distributions between these four water end-members, as shown in figures 3 and 4:

i) a mixing trend between DW and SW (or ESW-halite). Such a trend characterises the Delaware Basin and the reservoirs above the Triassic series in the Northern German Basin (Fig. 3A and B).

ii) mixing between DW and LiRB, as in the case of the Zagros, Amadeus, and Salinas basins and the Salton Trough (Fig. 3 C).

iii) mixing of LiRB with SW. These mixtures are typical of the Illinois and Appalachian basins (Fig. 3 D).

iv) a trend between ESW and LiRB. Such a trend was found in the reservoir in the basement below the Triassic series in the North German basin and Michigan, Mississippi Salt, North Louisiana Salt, Nepa Botuoba and Qaidam (deep wells) basins (Fig. 3 E and F).

### 3.2 *Li-enrichment in water end-members*

In a plot of Li versus Cl (Fig. 3), formation waters cover more than six orders of magnitude in Li concentrations, ranging from a few mg.l<sup>-1</sup> to ca. 1,000 mg.l<sup>-1</sup>, as well as in Cl content which ranges from a few mg.l<sup>-1</sup> to a few hundred thousand mg.l<sup>-1</sup>. Lithium and chlorine are roughly correlated when considering all data available. However, the distribution of Li follows very distinct trends from one basin to another. The variations of Li concentrations evolve then between 10<sup>-3</sup> and a few mg.l<sup>-1</sup> in waters with low Cl content and between 10 and 1,000 mg.l<sup>-1</sup> in waters with the highest chlorine content, i.e., close to that of halite (NaCl) saturation (from 25°C to 100°C) for evaporated seawater.

The lowest salinity waters distribute in two sub-poles as shown in figure 3B: i) the most common low salinity pole, characterised by chlorinities between a few mg and  $10 \text{ mg.l}^{-1}$  close to the river and rain waters and a Li concentration ranging from  $10^{-3}$  to  $10^{-2} \text{ mg.l}^{-1}$ , a little above the concentration of rain and river waters, for instance in the Mesozoic aquifers from the North German basin, and Zagros and Amadeus basins (Fig. 3C). ii) a pole which is ten times more concentrated in Li than the previous one for the same chlorinity, such as in the Delaware basin with Li concentrations of  $10^{-1} \text{ mg.l}^{-1}$  for a chlorinity of around  $10 \text{ mg.l}^{-1}$  (Fig. 3A and B). Interestingly, the mixing trend DW-SW is located above the trend of seawater dilution by pure water. Therefore, the most representative low salinity waters have a significant Li enrichment factor of around 10 (100 in the case of the Delaware pole), compared to highly diluted seawater and rainwater (Fig. 3 B). For some basins such as Illinois or Appalachian, waters show a predominant LiRB type brine and a few products of probable mixing between LiRB and less saline end-member closer to seawater (Fig. 3D). The central data cluster is considered in the following sections. Still, mixed waters were not deleted from the data sets.

For the LiRB cluster, the chlorinities are high and close to the values of saturated water to halite. The Li concentrations cover a significant range, with some data well above those of evaporated seawater, mostly between 10 and  $800 \text{ mg.l}^{-1}$  (Fig. 3E and F). Thus, on both sides of the mixing trends, Li concentrations distribute over one to two orders of magnitude (Fig. 3E and F). Therefore, a mechanism independent of the Cl concentration favours the Li-enrichment.

### 3.3 Brine origin: halogen and stable isotope data

*The halogen data:* During the formation of evaporites, seawater evaporation results in the so-called "primary" brine, which precipitate successively gypsum and then halides. Primary brines are stored as fluid inclusions in halides or within rock microporosity. Evaporites may dissolve when in contact with recharge waters or seawater, giving rise to secondary brines. To discriminate between brines, the classical use of halogen ratios (Cl/Br ratio) allows differentiation between primary and secondary brines (Banks and Yardley, 1992; Fontes and Matray, 1993). Primary brines have a Cl/Br ratio below that of seawater due to chlorine depletion in brines during halite crystallisation. In reverse, Cl/Br ratio is very high in secondary brines, as halite dissolution does not release bromine.

The Cl/Br ratio in most basins is lower than Cl/Br seawater ratio suggesting their primary origin (Fig. 5A to D). A few basins are exceptions as their waters have Cl/Br ratio higher than seawater, up to 850, and are typical of secondary brines: i) the Illinois Basin and Delaware (Fig. 5 A and C), and ii) the

upper part of the North German Basin (Mesozoic reservoirs above the evaporites, Fig. 5A). In the latter example, low-salinity water enters the reservoir and dissolves the underlying evaporites and diapirs.

The most Li-enriched waters (LiRB pole) have Cl/Br ratios that are lower than seawater and close to those of primary halite or epsomite saturated brines (Fig. 5D). The high Li concentrations in the North German Basin (Rotliegend and the Upper Carboniferous formation waters located in the centre of the basin below the Triassic salt formations) (3,000 times the value of seawater) correspond well from the point of view of Cl/Br ratios to primary brines saturated with halite (Lüders et al., 2010). The Cl/Br ratios in North Louisiana salt, Mississippi salt and Michigan are distributed in a sub-parallel trend to that of seawater evaporation, with Li concentrations multiplied by a factor of nearly 10. In North Louisiana and Appalachian, the Cl/Br spread down to low values of around 30. The only notable exception is the Qaidam basin, where high Cl/Br values of approximately 1,000 indicate that the brines are most likely secondary. In Salton Trough waters, brines are also secondary as their high chlorinity results predominantly from halite dissolution.

*Stable isotope data:* they are partially available on the studied basins and help to decipher the fluid origin (Craig and Gordon, 1965). When the diluting end-member DW dominates formation waters (recharge meteoric fluid) and is not affected by intense high-temperature fluid-rock interaction, they retain the negative  $\delta^{18}\text{O}$  value of meteoric waters. Such an end-member is illustrated by the Delaware and North German (reservoir above Triassic formations) basin waters. In the latter, data points are distributed along the global meteoric water line (Craig, 1961) between -10 and -5‰ ( $\delta^{18}\text{O}$  (V-SMOW)) and -75 and -45‰ ( $\delta\text{D}$  (V-SMOW)) (Fig. 6).

Evaporated seawater typically shows  $\delta^{18}\text{O}$  and  $\delta\text{D}$  values ranging between seawater value (i.e. 0‰) and +10‰ at the gypsum saturation stage and +4 and -14‰, respectively, at halite precipitation stages (Knauth and Beeunas, 1986) (Fig. 6). Most considered LiRB basinal brines plot close to the seawater evaporation trend between -5 and +8‰ for  $\delta^{18}\text{O}$  and between -25 and +7‰ for  $\delta\text{D}$ , with shifts in  $\delta^{18}\text{O}$  and  $\delta\text{D}$  values specific to each basin. Illinois basinal brine values are between -4 and +2‰ for  $\delta^{18}\text{O}$  and between -35 and -10‰ for  $\delta\text{D}$ . Data from Salinas- Sureste and Zagros basins show a distribution of  $\delta^{18}\text{O}$  (between 0 and +13‰), and  $\delta\text{D}$  (between 5 and -35‰) mostly shifted from the seawater evaporation towards higher  $\delta^{18}\text{O}$  values. In the Qaidam basin, the trend evolves between the meteoric line and higher  $\delta^{18}\text{O}$  values (between -10 and +15‰) at much lower  $\delta\text{D}$  values (between -60/-45 and -26‰) than in the other basins. The atypical features of Qaidam waters have been already deduced from considering major cation relationships (see below).

The shift to positive  $\delta^{18}\text{O}$  in most LiRB basinal brines accounts for high-temperature fluid-rock interactions (Williams and McKibben, 1989), confirming the effects of temperature-promoted water-rock interactions, which modify both isotopic and chemical features.

#### 3.4 *Water-rock interactions: the cation data*

Relationships between Li concentrations and other cations are represented using Na/K and Na/Ca ratios, as these cations are sensitive to fluid-rock interactions in basins (Fig. 7 and 8). For LiRB brines, the Na/K ratio covers a wide range of values, from low values of 0.1 and around 200, all below the Na/K ratio of SW or ESW (Fig. 7D). Resulting trends specific to each basin, making complex the definition of the location end-member in terms of Na/K values. A relatively identical trend is found for the Mississippi and Michigan basins. The distribution in the North Louisiana basin is steeper and similar to that in the North German basin (lower part under salt). As in Illinois (Fig. 7C), the significant shift in Na/K values towards high values above 100 is due to Na release after halite dissolution and is symptomatic of secondary brines. In the Zagros basin (Fig. 7B), the Li-concentration range is vast, with lower values below those of seawater due to dilution at a sub-constant Na/K ratio. A similar situation is recorded in the upper part of the North German basin (Fig. 7A).

In most LiRB basinal brines, the Li concentration is anti-correlated to the Na/Ca ratio. The latter covers at least two orders of magnitude between 0.2 and 10, below the Na/Ca of seawater and evaporated seawater (Fig. 8D). For the Delaware and upper North German basins (Fig. 8A), the dilution trends between rainwater and seawater end-members cover a large Na/Ca range distinct from LiRB trends. In Zagros (Fig. 8B), the dilution trend starts from an end-member close to LiRB at sub-constant Na/Ca, which may indicate the buffer role of limestones on the Na/Ca ratio. Salinas-Sureste and Amadeus basin plot close to the other LiRB (Fig. 8A and B).

The behaviour of Mg is remarkable compared to Li, as positive correlations characterise many basins, with a slope of 1 similar to the dilution of evaporated seawater or, conversely, evaporation trends. In a given basin, the Mg/Li ratios span an extensive range of values but are constant (Fig. 9). The Mg/Li ratio is around 1,000 in the North German basin (Mesozoic reservoir) and in Delaware (Fig. 9A), 100 in Mississippi Salt, Michigan (Fig. 9D), and Appalachian (Fig. 9C), in between 10 and 100 in Zagros and Amadeus (Fig. 9B), 10 in Delaware and North German (Carboniferous-Permian reservoir) and close to 1 at Salton Trough. For basins in which the LiRB pole is dominant, Mg concentrations have much tighter ranges, mainly from 1,000 to 10,000  $\text{mg.l}^{-1}$ .

### 3.5 *The Li-temperature relationships*

It is well known that during fluid-rock interaction, the chemistry of the fluid is controlled by a series of mineral (silicate)-fluid equilibria, which in turn are a function of temperature (Arnórsson et al. 1983). Cation ratios such as Na/K (Giggenbach, 1988, Fournier 1979) or Na-K corrected from the influence of divalent cations (Ca-Mg) were used as geothermometers, assuming pseudo-equilibria between waters and main silicates. The positive correlation between temperature and Li concentrations is, in addition, at the origin of several geothermometric relationships, including Li (Na/Li (Fouillac and Michard, 1981, Verma and Santoyo, 1997) and Mg/Li (Kharaka and Mariner, 1989). As such relationships are of interest for interpreting the distribution of Li concentrations, a Na/Li versus Na/K diagram is presented in figure 10 with a report of the thermometric relationships.

In brines from Salinas-Sureste and Zagros basins (Fig. 10 B), where measurements are in the range of 80-150°C, a relatively good agreement is found with temperatures from the Na/Li versus Na/K relationships. Conversely, most Na/Li -Na/K pairs for Li-rich formation waters (LiRB) plot outside the thermometric line (Fig. 10D). In the Michigan basin, the high K and Li concentrations move around the trend towards the left. In contrast, high Na concentrations in secondary brine from North Louisiana Salt displace the trend towards the right-hand side of the diagram. The disagreement between calculated and measured temperatures and the excess in Na, Li or K is probably indicative of a lack of equilibrium between brines and host rocks and of a specific enrichment different from those which depend strictly on temperature. The data are close to the expected values for the Salton Trough reservoirs, characterised by high temperatures ranging from 200 to 350°C.

### 3.6 *Comparison with salar brines*

Salar waters were plotted in the Li-Cl diagram (Fig. 11A). Data distribute between the Li-enriched end-member (LiRB type) and a dilute end-member, with almost the same trend as that recorded in the Zagros basin (Fig. 3C). Therefore, the evaporation/dilution trend for salars is nearly superimposed onto the LiRB and the diluted water mixing trend. Remarkably, the Uyuni brine evolution curve mimics the seawater evaporation curve but with a shift of about two orders of magnitude in Li concentrations. The salar brines in the Altiplano and Puna regions are the only ones that do not show mixing or evaporation trends but predominant LiRB brine features, particularly in deep horizons. In the Puna plateau, surficial

brines have Li values ranging from 57 to 5790 mg.l<sup>-1</sup> (López Steinmetz et al., 2020; Lopez Steinmetz and Salvi, 2021). The brines of the salars have Mg/Li ratios ranging from 1 to 100, specific to each basin (Fig. 11B). Most waters from salars have relatively low Na/Ca ratios. Salars in the Altiplano (Uyuni basin) and Puna (Olaroz, Cauchari and Salinas Grandes basins) regions have higher Na/Ca ratios (Fig. 11 C). In the Li versus Na/K ratio (Fig. 11D), the two most enriched salar waters distribute along a similar trend to that obtained for LiRB from sedimentary basins, characterised by the decreasing Na/Ca ratio at decreasing Li content. Similarly, the trend of decreasing Li concentration at sub-constant Na/K corresponds most probably to mixing effects. Finally, the Cl/Br ratio (Fig. 11E) is relatively high in salar brines, similar to those from the Qaidam basin and the Salton Trough and falls within the secondary brine field.

#### 4. Discussion

In some of the considered basins, Li concentrations are correlated with fluid salinity because waters result from the mixing between a dilute end-member, which includes meteoric waters or their evolved products with brines. Almost all mixing rates are encountered in the Delaware, Salinas-Sureste, Zagros, and Amadeus basins. The high-Cl end-members, however, cover a wide range of Li concentrations distributed between the SW-ESW (halite) line and the LiRB, i.e. over more than two orders of magnitude above.

Most LiRB brines have chlorinities close to halite saturation and Li concentrations between 80 and 2,000 ppm, i.e. above Li concentrations produced by extreme evaporation of seawater (up to bischoffite or saturation). Thus, the Li concentration only increases from 0.18 to 5 mg.l<sup>-1</sup> during evaporation, i.e. an enrichment factor close to 10 up to halite saturation stage and from 0.18 to 25 mg.l<sup>-1</sup> during evaporation, i.e. an enrichment factor close to 100 up to bischoffite saturation stage (Fontes and Matray, 1993). Therefore, an additional enrichment factor is required to reach concentrations 10 to 100 times that of evaporated seawater. The high Li concentrations cannot result from seawater evaporation alone. Therefore, looking for a process other than evaporation is necessary to explain this Li enrichment.

##### 4.1. *The shared features of the basins dominated by Li-rich brines*

The main characteristics of Li-rich brines are: i) they are evaporitic primary brines; ii) they are still in equilibrium with halite as their Cl concentration is close to halite saturation at 25°C or above.

Salt tectonics is one of the main factors responsible for the expulsion of primary brines, particularly the leakage of fluid inclusions into the salt and the migration of fluid inclusions under the effect of the thermal gradient as the expulsion of fluids from micropores. For example, such a process occurred twice in the Pyrenees: first, during Cretaceous rifting, characterised by evaporite stretching under anomalous heat fluxes associated with mantle uplift, and second, during thrusting induced by compression. During these two events, primary brines were expelled from Triassic evaporites, as shown by paleofluids trapped as fluid inclusions (Cathelineau et al., 2021).

The presence of massive evaporite layers may be one of the most favourable factors in obtaining large volumes of primary brines for most of the basins examined. Diapirs are, in some cases, very abundant such as in the Gulf Coast (Mississippi and North Louisiana salt formations and Salinas -Sureste basin) but are also present in the Siberian platform (Nepa-Botuoba basin) or the North German basin. In Gulf Coast, compressive deformation and diapirism cause the salt of the Louann Formation to move for kilometres (up to ten kilometres), intersecting all sedimentary formations, as shown in seismic sections (Hudec et al., 2013 a and b). In the Zagros, the Gasharan formation is partly the result of the dissolution of the thick Hormuz salt formation, and salt tectonics leads to the sealing of the reservoirs (Liu et al., 2018). The amplitude of the movements recorded by the salt formations is significant and explains the widespread expulsion of primary brines into these basins. Brines, generated along deformation zones, then invade the proximal reservoirs.

In addition, brines must be preserved from dilution. This condition is fulfilled when the convection is limited, and the renewal of allochthonous dilute fluids is minimised. Under such conditions, the primary brines may be predominant. Therefore, the presence of primary brines unaffected by dilution constitutes the first positive factor. The selected Li-rich brine basins share similar lithologies (Table 2), particularly the intercalation in siliciclastic and carbonate formations of salt-bearing horizons, sometimes affected by diapirism (salt domes). The favourable factors, compared to other basins hosting evaporitic sequences, thus are: i) a process yielding to brine expulsion (compression, tectonics), and ii) the lack of significant dilute fluid inputs in the reservoirs found in the relatively stable platform or cratons.

#### *4.2. Temperature-dependent processes*

The temperature range of the processes that governed the Li enrichment, in the past or more recently, may be considered the third factor of Li enrichment. It is well known that Li concentration

increases with increasing depth and temperature (Chan and Kastner, 2000; James et al., 2003; Coffey et al., 2021; Dugamin et al., 2021). The relationships between Li and other cations (Na, K, Mg) broadly follow the general trends predicted by empirical geothermometers, implying that temperature is essential in controlling Li concentrations. However, the discrepancies observed between reliable thermometric data (in situ measurements and silica in solution) confirm the importance of additional sources of Li, such as the presence of evaporated seawater and the contribution of Li from enriched surrounding rocks.

### 4.3 *The Li source factor*

Li- enriched source rocks containing leachable source minerals represent a necessary condition for high Li concentrations above the SW evaporation trend. The Li concentration in formation waters could result from significant water-rock interaction with the host rock, either within the immediate sedimentary environments, notably siliciclastic reservoirs or the basement lithologies, as the basin fluids may enter and then exit the crystalline basement.

The Na/K ratio is sensitive to cation exchange and changes when Na silicates (plagioclase, Na amphibole in the basement) or K silicates (K feldspar, muscovite, illite, biotite) are dissolved. During fluid-rock interactions such as plagioclase albitisation (anorthite end-member loss), cation exchange, or calcite dissolution results in a significant Ca release which modifies the Na/Ca mass ratio. The two cation ratios indicate that LiRB waters underwent critical water-rock processes. The primary brines have a Na/K ratio close to SW or ESW between 10 and 100, and the Na/Ca between 0.1 and 10 is lower than SW due to large Ca gains. Water-rock interactions monitor both ratios. Therefore, a process that enhances a long-lived interaction of the primary brines with minerals acting as Li-source during brine migration and storage is required to obtain a substantial Li enrichment.

Several contexts may allow the release of Li from source minerals and its temporary incorporation into newly-formed phases such as clays or its direct release into solution (e.g. Seyfried et al., 1984; Chan et al., 1993; Zhang et al., 1998; Chan and Kastner, 2000; James and Palmer, 2000; Williams and Hervig, 2005; Scholz et al., 2010; Hoyer et al., 2015). Several sources may be considered (see Figure 12 and Table A in supplementary material) :

*Differentiated magmatic series:* Figure 12 shows that Li is increasingly abundant due to magmatic differentiation from a few ppm in the ultrabasic series to 10 to 75 ppm in granites. Among the plutonic rocks, differentiated peraluminous granites can contain several hundred ppm of Li, primarily in the micas

(200 to 2500 ppm) (Bea et al., 1994; Dostal and Chatterjee, 1995; Raimbault et al., 1995; Förster et al., 1999; Müller et al., 2006; Sokolova et al., 2011; Canosa et al., 2012; Chicharro et al., 2016; Wu et al., 2017, Monnier et al., 2022). Extreme enrichments are found in highly differentiated aplites (Raimbault et al., 1995; Frindt et al., 2004; Moreno et al., 2014) and pegmatites (Teng et al., 2006; Liu et al., 2010; Canosa et al., 2012; Maneta and Baker, 2019) with the highest Li contents in Li-rich micas (polyolithionite, lepidolite) up to 2-3 % Li, petalite, spodumene and Li-phosphates (amblygonite series). Highly differentiated surficial volcanic emissions are the second series of Li-rich magmatic rocks. Ignimbrites, obsidian glass, including atmospheric emissions (tuff, glassy tephra), display an extensive range of Li-concentrations from 10 and 560 ppm (Breiter, 2012; Benson et al., 2017; Castor and Henry, 2020).

*Sediments:* Supergene degradation of basement lithologies provides the detrital elements of siliciclastic formations in basins (sands and conglomerates), which may be enriched in Li, notably muscovites and biotites from two mica granites. Pre-existing Mg-phyllosilicates, such as phlogopite, can lead to the crystallisation of F- and Li-rich hectorites.

Lake deposits under a climate with high hygrometric variations allowing evaporation and the formation of brackish water up to alkaline brines is the second surface environment particularly suitable for crystallising Li-rich trioctahedral smectites. Although fibrous clays are not as common as smectites and kaolinites, significant amounts of Li (20 - 90 ppm Li in palygorskite and 370 - 1,000 ppm Li in sepiolites) are reported by Tardy et al. (1972). Sepiolites are formed in lagoon environments, often saline during dry periods, such as the large Spanish basins (Madrid basin). The Vilcavaro sepiolites contain between 100 and 800 ppm Li (Torrez-Ruiz et al., 1994; Cuevas et al., 2003).

*Marine carbonate environments:* They have the lowest Li concentrations, with median values between 1 and 50 ppm (Hoefs and Sywall, 1997; Chan et al., 1997; Huh et al., 1998; Chan and Kastner, 2000; Chan et al., 2006).

*Li-clays produced by volcanic glass alteration:* Volcanic aerial products may form specific layers during eruptions intercalated within sedimentary series. Alteration of volcanic tuffs by hydrothermal solutions leads to mixtures of montmorillonite and hectorite (Starkey and Mountjoy, 1973). The glass matrix hydrates when in contact with low salinity waters, releasing Li, which can be incorporated in clays (Friedman and Smith, 1958; Ellis et al., 2022). Some siliciclastic sedimentary formations are thus rich in Li (median values over 100 ppm) as hectorite, illite, saponite, stevensite, and sepiolite (Hortsman, 1957 and references therein, Tardy et al., 1972; Vigier et al., 2008). Di-octahedral smectites are generally poor in Li, although Li is a monovalent cation easily exchangeable in the interlayer site of dioctahedral smectites. However, its concentration in the interlayer remains low due to competition with other

monovalent cations (Na, K) at one or two orders of magnitude higher in water. By contrast, trioctahedral smectites contain the highest amounts of Li, notably hectorite (Brenner-Tourtelot and Glanzman, 1978; Starkey, 1982). Hectorite accounts for about 8% of global Li reserves (Evans, 2008).

*Pieces of evidence of potential source rocks in the studied basins:* The functioning of source rocks and their traceability are challenging to verify. Li extraction from proximal sources, such as volcanic rocks, Li-enriched clay formations (bentonite) or Li-phyllosilicates dispersed in siliciclastic rocks or the underlying crystalline basement, is necessary. But, the information about source rocks may lack in the local geological descriptions, and Li rock and mineral contents are generally unavailable. There are, however, some cases where potential source rocks may be invoked: i) in Appalachian, K-bentonites are described below the Marcellus shale formation. They could be witnesses of ancient volcanic glass, which are good candidates as Li-source; ii) volcanic mafic and felsic intrusions are described in the North German, Gulf Coast, and Salton Trough. Brines, in addition, may have interacted with pre-salt basement rocks, such as in the lower part of the North German reservoirs. Biotite and muscovite in granitic basement may act as potential source minerals, as already invoked in the Soultz-sous-Forêts geothermal field (Rhine graben) by Dugamin (2022).

*Exploitability:* The Mg/Li ratios between 10 and 100 in the LiRB brines are close to those encountered in salar brines. Such ratios are more favourable than those reaching 1000, relative to seawater, for which the separation of the two cations may be more complicated.

#### 4.4 *The Li- cycle in the crust*

Figure 13 summarises the cycle of Li through the crust. It shows: i) the mechanisms of primary enrichment by evaporation from marine or continental waters yielding marine evaporites on the one hand and salars on the other hand, ii) the formation of secondary brines by salt dissolution, iii) the release of primary brines occurring mainly by crushing of evaporites related to compressive tectonics and salt tectonics (diapir formation), iv) the Li enrichment of primary brines by interaction with lithologies containing Li-rich minerals. The early Li enrichment is generally acquired in the proximity of salt layers (halite saturation) through water-rock interactions preserved from the entrance of low salinity recharge waters. Water-rock interactions may occur at medium to high temperatures for a basin in the case of geothermal activity, mainly when abnormal heat flows are linked to lithospheric thinning during rifting.

The favourable factors for secondary Li enrichment are the presence of: i) highly differentiated rocks (granites and pegmatites within the crystalline basement), ii) late magmatic dykes and intrusive sills in the basement and sedimentary basins, iii) detrital Li-rich minerals (muscovite in particular) in the siliciclastic formation, iv) sedimentary layers dominated by products of hydrothermal alteration or weathering of volcanic emission products from differentiated magmas (bentonite, hectorite rich layers). Enhanced enrichment may then occur thanks to temperature-dependent dissolution reactions involving the Li-bearing phases cited above. In the case of the Clayton Valley, Coffey et al. (2021) show that hydrothermal fluids interacting with volcanic tuffs may produce Li-rich brines, validating water-rock interactions as the primary driver for Li-enrichment.

## 5. Conclusion

Thirteen basins documented in the literature were selected for their representativeness of basinal brines. The main mechanisms controlling the geochemistry of the Li- enriched brines are as follows:

1- Lithium is correlated with Cl in a series of basins where mixing processes between a dilute end-member close to low-salinity water and a saline end-member relative to seawater or evaporated seawater (the Cl content being fixed by halite saturation) predominate. The dilute end-member has chemical and isotopic features close to meteoric waters, confirming that it corresponds to recharge waters. In Li-rich brines, at a sub-constant chlorinity fixed by the halite saturation, Li spans two orders of magnitude from 80 to 2000 mg.l<sup>-1</sup>, thus much above the Li concentrations resulting from seawater evaporation. The Li-rich brines were preserved from dilution.

2- Li-rich brines are primary evaporite brines close to halite saturation, with low Cl/Br ratios and  $\delta^{18}\text{O}$  similar to or higher than seawater. Favourable geological factors required to obtain such brines are: (i) brine expulsion from evaporites during tectonic events such as compression or salt tectonics; (ii) a relatively short migration distance to the reservoir; (iii) the absence of convection stimulated by thermal anomalies and of connection of reservoirs to recharge zones and surface-related faults to limit dilution processes. Increased Li concentrations can be achieved if primary brines interact strongly with leachable Li source rocks or minerals such as volcanic rocks, Li-rich clay beds or detrital Li-rich phyllosilicates dispersed in siliciclastic rocks. Further enrichment could come from the inflow of Li-rich geothermal waters related to magmatic activities. iv) temperature is a final favourable factor as Li is preferably extracted from source rocks with increasing temperature, a phenomenon well known and expressed by

increased Li/Na ratio with temperature. Symmetrically, the unfavourable factors include: i) large meteoric inflows through boundary faults, ii) inflows into deep connected porous reservoirs, iii) low-temperature gradients, iv) absence of source rocks (series dominated by carbonate platform sediments) such as preserved evaporites, and v) absence of geological events stimulating primary brine expulsion.

3- In some instances, brines are of secondary origin and convect as they are subjected to extreme geothermal gradients. At Salton Trough, high temperatures stimulated the water-rock interactions with evaporites, while a potential magmatic Li contribution cannot be precluded.

4- The exploitability of Li depends on its concentrations and bulk water chemistry. The Li-Mg plots show that the Mg/Li ratios cover various values. The separation of Li from Mg is easier for waters having Mg/Li ranging in between 10 and 100 ratios similar to those of solar brines than for waters with higher Mg/Li ratios.

### **Acknowledgements**

TotalEnergies financed the PhD thesis of Elza Dugamin through a CREGU contract. T. Elan, J.-P. Girard and E. Gaucher (TotalEnergies) are warmly thanked for fruitful discussions during the work. Two anonymous reviewers are thanked for their constructive comments which improved significantly the manuscript.

### **Competing interests**

The authors declare no competing interests.

### **References**

- Alexeev, S.V., Alexeeva, L.P., Vakhromeev, A.G., 2020. Brines of the Siberian Platform (Russia): geochemistry and processing prospects. *Appl. Geoch.* 117, 104588.
- Andrew, A.S., Whitford, D.J., Berry, M.D., Barclay, S.A., Giblin, A.M., 2005. Origin of salinity in produced waters from the palm valley gas field, northern territory, Australia. *Appl. Geoch.* 20, 727-747.
- Arnórsson, S., Gunnlaugsson, E., Svavarsson, H., 1983. The chemistry of geothermal waters in Iceland. III. Chemical geothermometry in geothermal investigations. *Geochim. Cosmochim. Acta* 47, 567-577.

- Bagheri, R., Nadri, A., Raeisi, E., Eggenkamp, H.G.M., Kazemi, G.A., Montaseri, A., 2014a. Hydrochemical and isotopic ( $\delta^{18}\text{O}$ ,  $\delta^2\text{H}$ ,  $87\text{Sr}/86\text{Sr}$ ,  $\delta^{37}\text{Cl}$  and  $\delta^{81}\text{Br}$ ). Evidence for the origin of saline formation water in a gas reservoir. *Chem. Geol.* 384, 62-75.
- Bagheri, R., Nadri, A., Raeisi, E., Kazemi, G.A., Eggenkamp, H.G.M., Montaseri, A., 2014b. Origin of brine in the Kangan gasfield: isotopic and hydrogeochemical approaches. *Environ. Earth Sci.* 72, 1055-1072.
- Banks, D.A., Yardley, B.W.D., 1992. Crush-leach analysis of fluid inclusions in small natural and synthetic samples. *Geochim. Cosmochim. Acta* 56, 245-248.
- Bea, F., Pereira, M.D., Corretgé, L.G., Fershtater, G.B., 1994. Differentiation of strongly peraluminous, perphosphorus granites: The Pedrobernardo pluton, central Spain. *Geochim. Cosmochim. Acta* 58, 2609-2627.
- Benson, T.R., Coble, M.A., Rytuba, J.J., Mahood, G.A., 2017. Lithium enrichment in intracontinental rhyolite magmas leads to Li deposits in caldera basins. *Nat. Commun.* 8, 1-9.
- Bibienne, T., Magnan, J.F., Rupp, A., Laroche, N., 2020. From mine to mind and mobiles: Society's increasing dependence on lithium. *Elements* 16, 265-270.
- Birkle, P., García, B.M., Padrón, C.M.M., 2009a. Origin and evolution of formation water at the Jujo-Tecominoacán oil reservoir, Gulf of Mexico. Part 1: Chemical evolution and water-rock interaction. *Appl. Geoch.* 24, 543-554.
- Birkle, P., García, B.M., Padrón, C.M.M., Eglington, B.M., 2009b. Origin and evolution of formation water at the Jujo-Tecominoacán oil reservoir, Gulf of Mexico. Part 2: Isotopic and field-production evidence for fluid connectivity. *Appl. Geoch.* 24, 555-573.
- Blondes, M.S., Shelton, J.L., Engle, M.A., Trembly, J.P., Doolan, C.A., Jubb, A.M., Chenault, J.C., Rowan, E.L., Haefner, R.J., Mailot, B.E., 2020. Utica shale play oil and gas brines: Geochemistry and factors influencing wastewater management. *Environ. Sci. Tech.* 54, 13917-13925.
- Bodine, M., Jones B., 1990. Normative analysis of groundwaters from the Rustler Formation associated with the Waste Isolation Pilot Plant (WIPP), Southeastern New Mexico. *The Geochemical Society Special Publication* 2, 213-269.
- Boiron, M.C., Cathelineau, M., Richard, A., 2010. Fluid flows and metal deposition near basement/cover unconformity: lessons and analogies from Pb-Zn-F-Ba systems for the understanding of Proterozoic U deposits. *Geofluids* 10, 270-292.
- Bradley, D.C., Stillings, L.L., Jaskula, B.W., Munk, L., McCauley, A.D., 2017. Lithium, Chapter K. Schulz, K.J., DeYoung, Jr. J.H., Seal II, R.R., Bradley, D.C. (eds.). *Critical mineral resources of the United States* –

Economic and environmental geology and prospects for future supply U.S. Geological Survey Professional Paper 1802, K1–K21.

- Breiter, K., 2012. Nearly contemporaneous evolution of the A- and S-type fractionated granite in the Krušné hory/Erzgebirge Mts., Central Europe. *Lithos* 151, 105-121.
- Brenner-Tourtelot, E.F., Glanzman, R.K., 1978. Lithium-bearing rocks of the horse spring formation, Clark County, Nevada. *Energy* 3, 255-262.
- Canosa, F., Martin-Izard, A., Fuertes-Fuente, M., 2012. Evolved granitic systems as a source of rare-element deposits: The Ponte Segade case (Galicia, NW Spain). *Lithos* 153, 165-176.
- Carpenter, A.B., 1978. Origin and chemical evolution of brines in sedimentary basins. SPE Annual Fall Technical Conference and Exhibition, Houston, Texas, October 1978. Paper SPE-7504-MS.
- Carpenter, A.B., Trout, M.L., Pickett, E.E., 1974. Preliminary report on the origin and chemical evolution of lead- and zinc-rich oil field brines in Central Mississippi. *Econ. Geol.* 69, 1191- 1206.
- Castor, S.B., Henry, C.D., 2020. Lithium-Rich Claystone in the McDermitt Caldera, Nevada, USA: Geologic, Mineralogical, and Geochemical Characteristics and Possible Origin. *Minerals* 10, 68.
- Cathelineau, M., Boiron, M.C., Jakomulski, H., 2021. Triassic evaporites: a vast reservoir of brines mobilised successively during rifting and thrusting in the Pyrenees. *J. Geol. Soc.*, 178-6.
- Chan, L.H., Kastner, M., 2000. Lithium isotopic compositions of pore fluids and sediments in the Costa Rica subduction zone: implications for fluid processes and sediment contribution to the arc volcanoes. *Earth Planet. Sci. Lett.* 183, 275-290.
- Chan, L.H., Edmond, J.M., Thompson, G., 1993. A lithium isotope study of hot springs and metabasalts from mid-ocean ridge hydrothermal systems. *J. Geophys. Res. Solid Earth* 98, 9653-9659.
- Chan, L.H., Sturchio, N.C., Katz, A., 1997. Lithium isotope study of the Yellowstone hydrothermal system. *EOS Trans. Am. Geophys. Union* 78, F802.
- Chan, L.H., Leeman, W.P., Plank, T., 2006. Lithium isotopic composition of marine sediments. *Geochem. Geophys. Geosyst.* 7.
- Cheng, X., Zhang, D., Jolivet, M., Yu, X., Du, W., Liu, R., Guo, Z., 2018. Cenozoic structural inversion from transtension to transpression in Yingxiong Range, western Qaidam Basin: New insights into strike-slip superimposition controlled by Altyn Tagh and Eastern Kunlun Faults. *Tectonophysics* 723, 229-241.
- Chicharro, E., Boiron, M.C., Lopez-Garcia, J.A., Barfod, D.N., Villaseca, C., 2016. Origin, ore forming fluid evolution and timing of the Logrosán Sn- (W) ore deposits (Central Iberian Zone, Spain). *Ore Geol. Rev.* 72, 896-913.

- Coffey, D.M., Munk, L.A., Ibarra, D.E., Butler, K.L., Boutt, D.F., Jenckes, J., 2021. Lithium storage and release from lacustrine sediments: Implications for lithium enrichment and sustainability in continental brines. *Geochem. Geophys. Geosyst.* 22.
- Collins, A., 1975. *Geochemistry of oilfield waters*. First ed. Elsevier, Amsterdam.
- Comision Nacional de Hidrocarburos, 2015. Gulf of Mexico-Deep water-South sector. Saline basin: petroleum geological synthesis.
- Craig, H., 1961. Isotopic Variations in Meteoric Waters. *Science* 133, 1702–1703.
- Craig, H., Gordon, L. I., 1965. Deuterium and Oxygen 18 variations in the ocean and the marine atmosphere. in *Proceedings of a Conference on Stable Isotopes in Oceanographic Studies and Paleotemperatures*, Spoleto, July 26–27, E. Tongiorgi Ed., Lab. Geol.Nucl. Sci., Pisa, Italy, 9–130.
- Cuevas, J., de la Villa, R.V., Ramirez, S., Petit, S., Meunier, A., Leguey, S., 2003. Chemistry of Mg smectites in lacustrine sediments from the Vicalvaro sepiolite deposit, Madrid Neogene Basin (Spain). *Clays Clay Miner.* 51, 457-472.
- Davisson, M.L., Criss, R.E., 1996. Na-Ca-Cl relations in basinal fluids. *Geochim. Cosmochim. Acta* 60, 2743-2752.
- Demir, I., Seyler, B., 1999. Chemical Composition and Geologic History of Saline Waters in Aux Vases and Cypress Formations, Illinois Basin. *Aquat. Geochem.* 5, 281-311.
- Dostal, J., Chatterjee, A.K., 1995. Origin of topaz-bearing and related peraluminous granites of the Late Devonian Davis Lake pluton, Nova Scotia, Canada: crystal versus fluid fractionation. *Chem. Geol.* 123, 67-88.
- Dresel, P.E., Rose, A.W., 2010. *Chemistry and origin of oil and gas well brines in Western Pennsylvania: Pennsylvania, Geological Survey, 4th ser. OFOG 10–01.0 48.*
- Dugamin, E.J., Richard, A., Cathelineau, M., Boiron, M.C., Despinois, F., Brisset, A., 2021. Groundwater in sedimentary basins as potential lithium resource: a global prospective study. *Sci. Rep.* 11, 1-10.
- Dugamin, E.J., 2022. *Facteurs contrôlant les concentrations en métaux dans les eaux de formation des bassins sédimentaires*. PhD thesis, Lorraine University, 343p.
- Dugamin, E.J., Richard, A., Boiron, M.C., Cathelineau, M., Despinois, F., 2023. Controls on metal concentrations in sedimentary formation waters and fluid inclusions. *Earth Sc. Rev.* submitted.
- Ellis, B.S., Szymanowski, D., Harris, C., Tollan, P.M.E., Neukampf, J., Guillong, M., Cortes- Calderon, E.A., Bachmann, O., 2022. Evaluating the Potential of Rhyolitic Glass as a Lithium Source for Brine Deposits. *Econ. Geol.* 117, 91-105.

- Engle, M.A., Reyes, F.R., Varonka, M.S., Orem, W.H., Ma, L., Ianno, A.J., Schell, T. M., Xu, P., Carroll, K.C., 2016. Geochemistry of formation waters from the Wolfcamp and "Cline" shales: Insights into brine origin, reservoir connectivity, and fluid flow in the Permian Basin, USA. *Chem. Geol.* 425, 76-92.
- Ericksen, G.E., Salas O.R., 1987. Geology and resources of Salars in the Central Andes. U.S. Geological Survey Open-File Report, 88-210.
- Evans, R. 2008. An abundance of lithium. *Environmental Science*.
- Fontes, J.C., Matray, J.M., 1993. Geochemistry and Origin of Formation Brines from the Paris Basin, France 1. Brines associated with Triassic salts. *Chem. Geol.* 109, 149-175.
- Förster, H.J., Tischendorf, G., Trumbull, R.B., 1999. Late-Collisional Granites in the Variscan Erzgebirge, Germany. *J. Petrol.* 40, 1613-1645.
- Fouillac, C., Michard, G., 1981. Sodium/lithium ratios in water applied to geothermometry of geothermal reservoirs. *Geothermics* 10, 55-70.
- Fournier, R.O., 1979. A revised equation for the Na/K geothermometer. *Transactions of the Geothermal Resources Council*, 3, 221-224.
- Franco, M.G., Arnold, Y.J.P., Santamans, C.D., Steinmetz, R.L.L., Tassi, F., Venturi, S., Jofré, C.B., Caffè, P.J., Córdoba, F.E., 2020. Chemical and isotopic features of Li-rich brines from the Salar de Olaroz, Central Andes of NW Argentina. *J. South Am. Earth Sci.* 103, 102742.
- Friedman, I., Smith, R.L., 1958. The deuterium content of water in some volcanic glasses. *Geochim. Cosmochim. Acta* 15, 218-228.
- Frindt, S., Haapala, I., Pakkanen, L., 2004. Anorogenic Gross Spitzkoppe granite stock in central western Namibia: Part I. Petrology and geochemistry. *Am. Mineral.* 89, 841-856.
- Giggenbach, W.F., 1988. Geothermal solute equilibria. Derivation of Na-K-Mg-Ca geothermometers. *Geochim. Cosmochim. Acta* 52, 2749-2765.
- Hanor, J.S., 1987. Origin and migration of subsurface sedimentary brines. *SEPM short course* 21, 247.
- Hoefs, J., Sywall, M., 1997. Lithium isotope composition of Quaternary and Tertiary biogenic carbonates and a global lithium isotope balance. *Geochim. Cosmochim. Acta* 61, 2679- 2690.
- Horstman, E.L., 1957. The distribution of lithium, rubidium and caesium in igneous and sedimentary rocks. *Geochim. Cosmochim. Acta* 12, 1-28.
- Hoyer, M., Kummer, N.A., Merkel, B., 2015. Sorption of lithium on bentonite, kaolin and zeolite. *Geosciences* 5, 127-140.
- Hudec, M.R., Jackson, M.P., Peel, F.J., 2013a. Influence of deep Louann structure on the evolution of the northern Gulf of Mexico Salt Influence. *Am. Ass. Pet. Geol. Bull.* 97, 1711- 1735.

- Hudec, M.R., Norton, I.O., Jackson, M.P., Peel, F.J., 2013b. Jurassic evolution of the Gulf of Mexico salt basin. *Am. Ass. Pet. Geol. Bull.* 97, 1683-1710.
- Huh, Y., Chan, L.H., Zhang, L., Edmond, J.M., 1998. Lithium and its isotopes in major world rivers: implications for weathering and the oceanic budget. *Geochim. Cosmochim. Acta* 62, 2039-2051.
- Hulen, J.B., Kaspereit, D., Norton, D.L., Osborn, W., Pulka, F.S., Bloomquist, R., 2002. Refined conceptual modeling and a new resource estimate for the Salton Sea geothermal field, Imperial Valley, California. *Geothermal Resources Council Transactions* 26, 22-25.
- Jahani, S., Callot, J.P., Letouzey, J., Frizon de Lamotte, D., 2009. The eastern termination of the Zagros Fold-and-Thrust Belt, Iran: Structures, evolution, and relationships between salt plugs, folding, and faulting. *Tectonics* 28.
- James, R.H., Palmer, M.R., 2000. Marine geochemical cycles of the alkali elements and boron: The role of sediments. *Geochim. Cosmochim. Acta* 64, 3111-3122.
- James, R.H., Allen, D.E., Seyfried Jr, W.E., 2003. An experimental study of alteration of oceanic crust and terrigenous sediments at moderate temperatures (51 to 350°C): Insights as to chemical processes in near-shore ridge-flank hydrothermal systems. *Geochim. Cosmochim. Acta* 67, 681-691.
- Jarrett, A., Edwards, D., Boreham, C., McKirdy, D., 2016. Petroleum geochemistry of the Amadeus Basin. Annual Geoscience Exploration Seminar (AGES) Proceedings. Alice Springs. Northern Territory Geological Survey Record 2016-001, 37-42.
- Kharaka, Y.K., Mariner, R.H., 1989. Chemical geothermometers and their application to formation waters from sedimentary basins. In: Naeser, N.D., McCulloh, T.H. (eds) *Thermal history of sedimentary basins*. Springer, New York, NY.
- Kharaka, Y.K., Hanor, J.S., 2003. Deep Fluids in the Continents: I. Sedimentary Basins. Drever, J.L. (ed.) *Treatise on geochemistry* 5, 1-48.
- Kharaka, Y.K., Maest, A.S., Carothers, W.W., Law, L.M., Lamothe, P.J., Fries, T.L., 1987. Geochemistry of metal-rich brines from Central Mississippi Salt Dome Basin, USA. *Appl. Geoch.* 2, 543-561.
- Kloppmann, W., Négrel, P., Casanova, J., Klinge, H., Schelkes, K., Guerrot, C., 2001. Halite dissolution derived brines in the vicinity of a Permian Salt Dome (N German Basin). Evidence from boron, strontium, oxygen, and hydrogen isotopes. *Geochim. Cosmochim. Acta* 65, 4087-4101.
- Knauth, L.P., Beeunas, M.A., 1986. Isotope geochemistry of fluid inclusions in Permian halite with implications for the isotopic history of ocean water and the origin of saline formation waters. *Geochim. Cosmochim. Acta* 50, 419-433.

- Kumar, A., Fukuda, H., Hatton, T.A., Lienhard, J.H., 2019. Lithium recovery from oil and gas Produced water: A need for a growing energy industry. *Energy Letters* 4(6), 1471-1474
- Labbe, J.F., Daw, G., 2012. Panorama 2011 du marché du lithium. BRGM RP-61340-FR
- Land, L.S., 1995. Na-Ca-Cl saline formation waters, Frio Formation (Oligocene), South Texas, USA: products of diagenesis. *Geochim. Cosmochim. Acta* 59, 2163-2174.
- Land, L.S., Prezbindowski, D.R., 1981. The origin and evolution of saline formation water, Lower Cretaceous carbonates, south-central Texas, USA. *J. Hydrol.* 54, 51-74.
- Land, L.S., Macpherson, G.L., 1992. Origin of saline formation waters, Cenozoic section, Gulf of Mexico sedimentary basin. *Am. Ass. Pet. Geol. Bull.* 76, 1344-1362.
- Land, L.S., Kupecz, J.A., Mack, L.E., 1988. Louann salt geochemistry (Gulf of Mexico sedimentary basin, USA): a preliminary synthesis. *Chem. Geol.* 74, 25-35.
- Lippmann, M., Truesdell, A., Frye, G., 1999. The Cerro Prieto and Salton Sea geothermal fields—Are they really alike. In *Proceedings of the 24th Workshop on Geothermal Reservoir Engineering*, Stanford University, Stanford, California, 25-27.
- Liu, X.M., Rudnick, R.L., Hier-Majumder, S., Sirbescu, M.L.C., 2010. Processes controlling lithium isotopic distribution in contact aureoles: A case study of the Florence County pegmatites, Wisconsin. *Geochem. Geophys. Geosyst.* 11-8.
- Liu, X., Wen, Z., Wang, Z., Song, C., He, Z., 2018. Structural characteristics and main controlling factors on petroleum accumulation in Zagros Basin, Middle East. *J. Nat. Gas Geosci.* 3, 273-281.
- López Steinmetz, R.L., Salvi, S., Garcia, G., Arnold, Y.P., Beziat, D., Franco, G., Constantini, G., Cordoba, F.E., Caffè, P.J., 2018. Northern Puna Plateau-scale survey of Li brine-type deposits in the Andes of NW Argentina. *J Geoch. Explor.* 190, 26-38.
- López Steinmetz, R.L., Salvi, S., Sarchi, C., Santamans, C., López Steinmetz, L.C., 2020. Lithium and brine geochemistry in the salars of the Southern Puna, Andean Plateau of Argentina. *Econ. Geol.* 115, 1079-1096.
- López Steinmetz, R.L., Salvi, S., 2021. Brine grades in Andean salars: When basin size matters A review of the lithium triangle. *Earth Sc. Rev.* 217, 103615.
- Lowenstein, T.K., Hardie, L.A., Timofeeff, M.N., Demicco, R.V., 2003. Secular variation in seawater chemistry and the origin of calcium chloride basinal brines. *Geology.* 31, 857-860.

- Lüders, V., Plessen, B., Romer, R. L., Weise, S. M., Banks, D. A., Hoth, P., Dulski, P., Schettler, G., 2010. Chemistry and isotopic composition of Rotliegend and Upper Carboniferous formation waters from the North German Basin. *Chem. Geol.* 276, 198-208.
- Ma, Z., Han, F., Chen, T., Yi, L., Lu, X., Chen, F., Liu, X., Yuan, W., 2021. The Forming Age and the Evolution Process of the Brine Lithium Deposits in the Qaidam Basin Based on Geochronology and Mineral Composition. *Front. Earth Sci.* 9, 702223.
- Maneta, V., Baker, D.R., 2019. The potential of lithium in alkali feldspars, quartz, and muscovite as a geochemical indicator in the exploration for lithium-rich granitic pegmatites: A case study from the spodumene-rich Moblan pegmatite, Quebec, Canada. *J. Geochem. Explor.* 205, 106336.
- McCaffrey, M.A., Lazar, B.H.D.H., Holland, H.D., 1987. The evaporation path of seawater and the coprecipitation of Br (super-) and K (super+) with halite. *J. Sed. Res.* 57, 928-937.
- Mempes, M., Cremasco, D., Hansberry, R., 2020. Geology and evolution of the Dukas structure, Amadeus Basin, Northern Territory. *Annual Geoscience Exploration Seminar (AGES) Proceedings, Alice Springs, Northern Territory* 90.
- Mohr, S., Mudd, G., Giurco, D., 2010. Lithium resources and production: A critical global assessment. (Institute for Sustainable Futures (University of Technology, Sydney) and Department of Civil Engineering (Monash University)).
- Moldovanyi E.P., Walter, L.M., 1992. Regional trends in water chemistry, Smackover Formation, Southwest Arkansas: geochemical and physical controls. *Am. Ass. Pet. Geol. Bull.* 76, 864-894.
- Monnier, L., Salvi, S., Melleton, J., Lach, P., Pochon, A., Bailly, L., Beziat, D., De Parseval, P., 2022. Mica trace-element signatures: Highlighting superimposed W-Sn mineralisations and fluid sources. *Chem. Geol.* 600, 120866.
- Moreno, J.A., Molina, J.F., Montero, P., Anbar, M.A., Scarrow, J.H., Cambeses, A., Bea, F., 2014. Unraveling sources of A-type magmas in juvenile continental crust: Constraints from compositionally diverse Ediacaran post-collisional granitoids in the Katerina Ring Complex, southern Sinai, Egypt. *Lithos* 192, 56-85.
- Morton, R.A., Land, L.S., 1987. Regional variations in formation water chemistry, Frio formation (Oligocene), Texas Gulf Coast. *Am. Ass. Pet. Geol. Bull.* 71, 191-206.
- Mount, V.S., 2014. Structural style of the Appalachian Plateau fold belt, north-central Pennsylvania. *Journal of Structural Geology* 69, 284-303.

- Müller, A., Seltmann, R., Halls, C., Siebel, W., Dulski, P., Jeffries, T., Spratt, J., Kronz, A., 2006. The magmatic evolution of the Land's End pluton, Cornwall, and associated pre- enrichment of metals. *Ore Geol. Rev.* 28, 329-367.
- Munk, L.A., Hynek, S., Bradley, D.C., Boutt, D., Labay, K.A., Jochens H., 2016. Lithium brines: A global perspective, *Econ. Geol.* 18, 339–365.
- Nate, S., Bilan, Y., Kurylo, M., Lyashenko, O., Napieralski, P., Kharlamova, G., 2021. Mineral Policy within the Framework of Limited Critical Resources and a Green Energy Transition. *Energies* 14, 2688.
- Qishun, F., Ma, H., Lai, Z., Tan, H. Li, T., 2010. Origin and evolution of oilfield brines from Tertiary strata in Western Qaidam Basin: constraints from  $^{87}\text{Sr}/^{86}\text{Sr}$ ,  $\delta\text{D}$ ,  $\delta^{18}\text{O}$ ,  $\delta^{34}\text{S}$  and water chemistry. *Chin. J. Geochem.* 29, 446-54.
- Raimbault, L., Cuney, M., Azencott, C., Duthou, J.L., Joron, J.L., 1995. Geochemical evidence for a multistage magmatic genesis of Ta-Sn-Li mineralisation in the granite at Beauvoir, French Massif Central. *Econ. Geol.* 90, 548-576.
- Rine, M.J., 2015. Depositional facies and sequence stratigraphy of Niagaran-lower salina reef complex reservoirs of the Guelph formation, Michigan Basin. Master Theses, Western Michigan University.
- Risacher, F., Fritz, B., 1991. Quaternary geochemical evolution of the salars of Uyuni and Coipasa, Central Altiplano, Bolivia. *Chem. Geol.* 90, 211-31.
- Risacher, F., Alonso, H., Salazar, C., 1999. Geoquímica de aguas en cuencas cerradas, I, II, III Regiones, Chile. Ministerio de Obras Publicas, Direccion General de Aguas. Technical Report S.I.T. 51.
- Rogers, J.D., Boutwell, G., Watkins, C., Karadeniz, D., 2006. Chapter Three: Geology of the New Orleans Region. Independent Levee, Investigation Team, New Orleans Levee Systems, Hurricane Katrina.
- Sanders, L.L., 1991. Geochemistry of Formation Waters from the Lower Silurian Clinton Formation (Albion Sandstone), Eastern Ohio. *The American Association of Petroleum Geologists Bulletin* 75, 1593-1608.
- Sanjuan, B., Millot, R., Dezayes, C. Brach, M., 2010. Main characteristics of the deep geothermal brine (5km) at Soultz-sous-Forêts (France) determined using geochemical and tracer test data. *C. R. Geosci.* 342, 546-559.
- Sanjuan, B., Gourcerol, B., Millot, R., Rettenmaier, D., Jeandel, E., Rombaut, A., 2022. Lithium-rich geothermal brines in Europe: An up-date about geochemical characteristics and implications for potential Li resources. *Geothermics* 101, 102385.
- Scholz, F., Hensen, C., De Lange, G.J., Haeckel, M., Liebetrau, V., Meixner, A., Reitz, A., Romer, R.L., 2010. Lithium isotope geochemistry of marine pore waters—insights from cold seep fluids. *Geochim. Cosmochim. Acta* 74, 3459-3475.

- Seyfried Jr, W.E., Janecky, D.R., Mottl, M.J., 1984. Alteration of the oceanic crust: implications for geochemical cycles of lithium and boron. *Geochim. Cosmochim. Acta* 48, 557-569.
- Skeen, J.C., 2010. Basin analysis and aqueous chemistry of fluids in the Oriskany Sandstone, Appalachian Basin, USA. Graduate Theses, Dissertations, and Problem Reports, 2978.
- Smith, L.B., 2013. Shallow transgressive onlap model for Ordovician and Devonian organic- rich shales, New York State. SPE/AAPG/SEG Unconventional Resources Technology Conference. OnePetro.
- Sokolova, E.N., Smirnov, S.Z., Astrelina, E.I., Annikova, I.Y., 2011. Ongonite - elvan magmas of the Kalguty ore-magmatic system (Gorny Altai): composition, fluid regime, and genesis. *Russ. Geol. Geophy.* 52, 1378-1400.
- Starkey, H.C., 1982. The role of clays in fixing lithium. US Government Printing Office 1278.
- Starkey, H.C., Mountjoy, W., 1973. Identification of a lithium-bearing smectite from Spor Mountain, Utah. *J. Res. U S Geol. Surv.* 1, 415-419.
- Stueber, A.M., Walter, L.M., 1991. Origin and chemical evolution of formation waters from Silurian-Devonian strata in the Illinois Basin, USA. *Geochim. Cosmochim. Acta* 55, 309-325.
- Stueber, A.M., Walter, L.M., Huston, T.J., Pushkar, P., 1993. Formation waters from Mississippian-Pennsylvanian reservoirs, Illinois Basin, USA: Chemical and isotopic constraints on evolution and migration. *Geochim. Cosmochim. Acta* 57, 763-784.
- Tardy, Y., Krempf, G., Trauth, N., 1972. Le lithium dans les minéraux argileux des sédiments et des sols. *Geochim. Cosmochim. Acta* 36, 397-412.
- Tan, H., Rao, W., Ma, H., Chen, J., Li, T., 2011. Hydrogen, oxygen, helium and strontium isotopic constraints on the formation of oilfield waters in the Western Qaidam Basin, China. *J. Asian Earth Sc.* 40, 651-660.
- Teng, F.Z., McDonough, W.F., Rudnick, R.L., Walker, R.J., Sirbescu, M.L.C., 2006. Lithium isotopic systematics of granites and pegmatites from the Black Hills, South Dakota. *Am. Mineral.* 91, 1488-1498.
- Thompson, J.M., Fournier, R.O., 1988. Chemistry and geothermometry of brine produced From the Salton Sea scientific drill hole, Imperial Valley, California. *Journal of Geophysical Research: Solid Earth* 93, 13165-13173.
- Torres-Ruiz, J., López-Galindo, A., González-López, J.M., Delgado, A. 1994. Geochemistry of Spanish sepiolite-palygorskite deposits: genetic considerations based on trace elements and isotopes. *Chem. Geol.* 112, 221-245
- Ulmishek, G.F., 2001. Petroleum geology and resources of the Nepa-Botuoba high, Angara- Lena terrace, and Cis-Patom foredeep, Southeastern Siberian craton, Russia. US Department of the Interior, US Geological Survey.

- U.S. Geological Survey., 2021. Mineral commodity summaries. U.S. Geological Survey.
- Verma, S.P., Santoyo, E., 1997. New improved equations for NaK, NaLi and SiO<sub>2</sub> geothermometers by outlier detection and rejection. *J. Volcanol. Geotherm. Res.* 79, 9-23.
- Vigier, N., Decarreau, A., Millot, R., Carignan, J., Petit, S., France-Lanord, C., 2008. Quantifying Li isotope fractionation during smectite formation and implications for the Li cycle. *Geochim. Cosmochim. Acta* 72, 780-792.
- White, D.E., 1965. Saline waters of sedimentary rocks. In: *Fluids in Subsurface Environments*. Yound A. and Galley G.E. (eds.), *Am. Ass. Petrol. Geol. Mem.*, 4, 342–366.
- Williams, A.E., McKibben, M.A., 1989. A brine interface in the Salton Sea geothermal system, California: fluid geochemical and isotopic characteristics. *Geochim. Cosmochim. Acta* 53, 1905-1920.
- Williams, L.B., Hervig, R.L., 2005. Lithium and boron isotopes in illite-smectite: The importance of crystal size. *Geochim. Cosmochim. Acta* 69, 5705–5716.
- Wilson, T.P., Long, D.T., 1993a. Geochemistry and isotope chemistry of Ca-Na-Cl brines in Silurian strata, Michigan Basin, USA. *Appl. Geoch.* 8, 507-524
- Wilson, T.P., Long, D.T., 1993b. Geochemistry and isotope chemistry of Michigan Basin brines: Devonian formations. *Appl. Geoch.* 8, 81-100.
- Wu, M., Samson, I.M., Zhang, D., 2017. Textural and chemical constraints on the formation of disseminated granite-hosted W-Ta-Nb mineralisation at the Dajishan Deposit, Nanling Range, Southeastern China. *Econ. Geol.* 112, 855-887.
- Yaksic, A., Tilton, J.E., 2009. Using the cumulative availability curve to assess the threat of mineral depletion: The case of lithium. *Resources Policy* 34, 185-194
- Zhang, L., Chan, L.H., Gieskes, J.M., 1998. Lithium isotope geochemistry of pore waters from Ocean Drilling Program Sites 918 and 919, Irminger Basin. *Geochim. Cosmochim. Acta* 62, 2437-2450.
- Zhang, P.X., 1987. *The Salt Lakes of the Qaidam Basin*. Beijing: Science Press.
- Zhang, R., Ghosh, R., Sen, M.K., Srinivasan, S., 2013. Time-lapse surface seismic inversion with thin bed resolution for monitoring CO<sub>2</sub> sequestration: A case study from Cranfield, Mississippi. *Int. J. Greenhouse Gas Control* 18, 430-438.

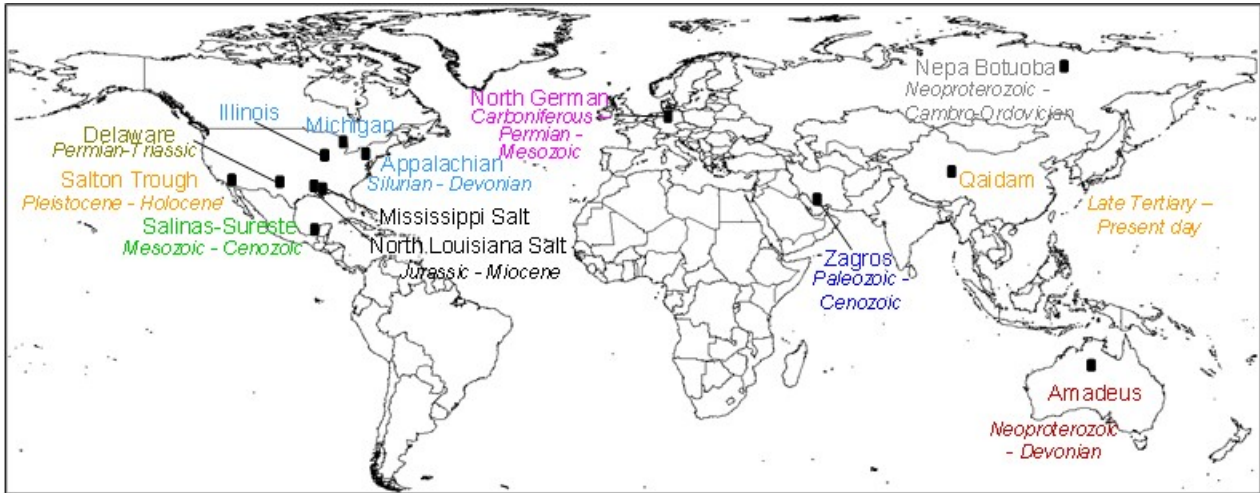


Fig. 1. World map showing the 13 sedimentary basins selected for this study. The age of each sedimentary basin is specified in italics and is indicated by different colours.

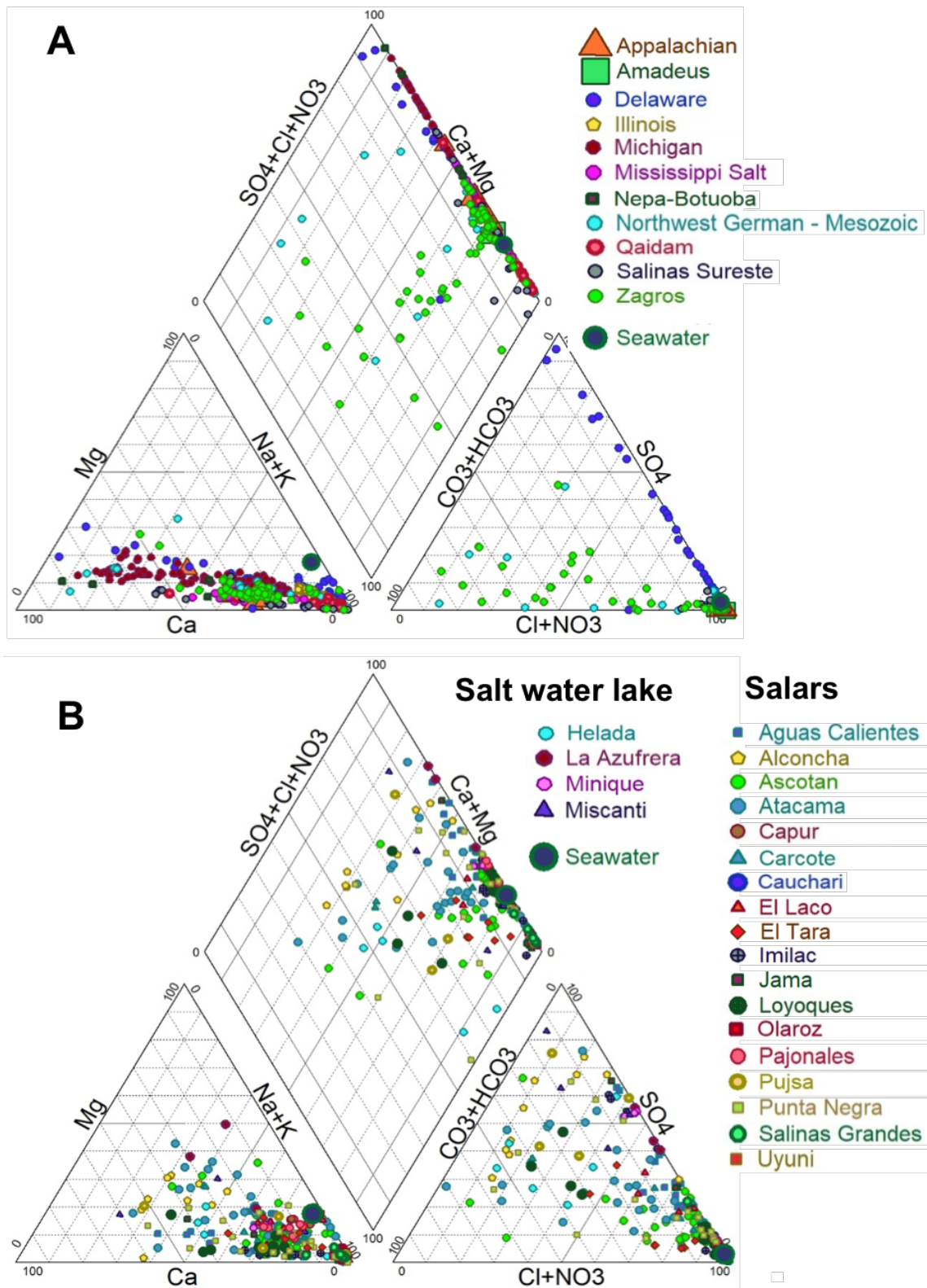


Fig. 2. Piper diagram applied to waters from sedimentary reservoirs (A) and closed basins (B). Data were compiled from literature (see references in table 1 and 3).

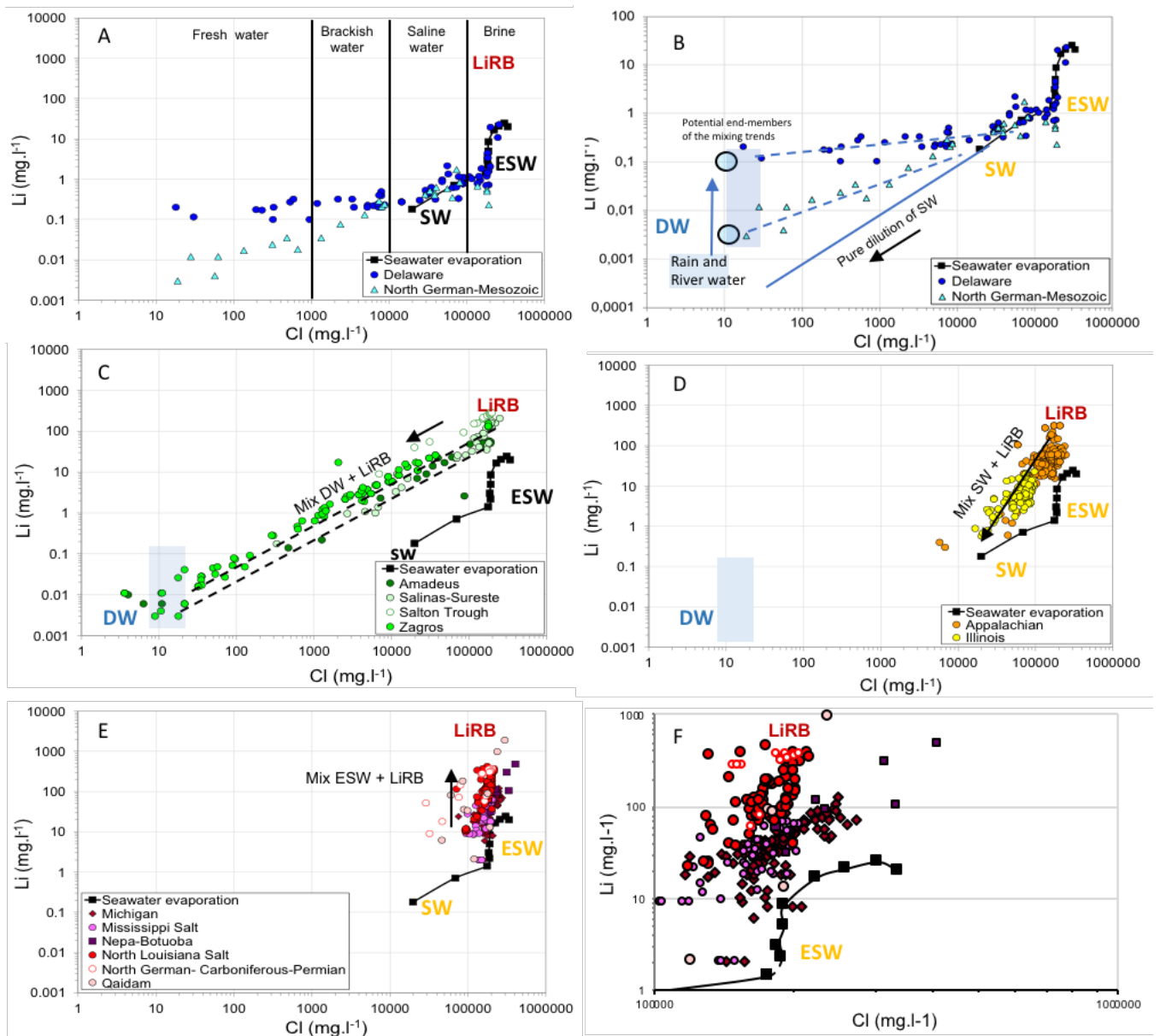


Fig. 3. Lithium concentration in sedimentary formation waters as a function of chloride concentration. DW: dilute water, SW: Seawater, ESW: evaporated sea water, LiRB: Li rich brine. Data for basins with extended dilution trends of seawater are in A, B and C, with B an enlarged and commented version of A. Boundaries between fresh, saline, brackish waters and brines are from Carpenter (1978). D corresponds to sets of brines enriched in Li with a mixing trend towards seawater, and E shows the brines with the highest Li enrichment in between 10 and 100 times the Li content of evaporated seawater. F is an enlarged version of E to show details of data distribution.

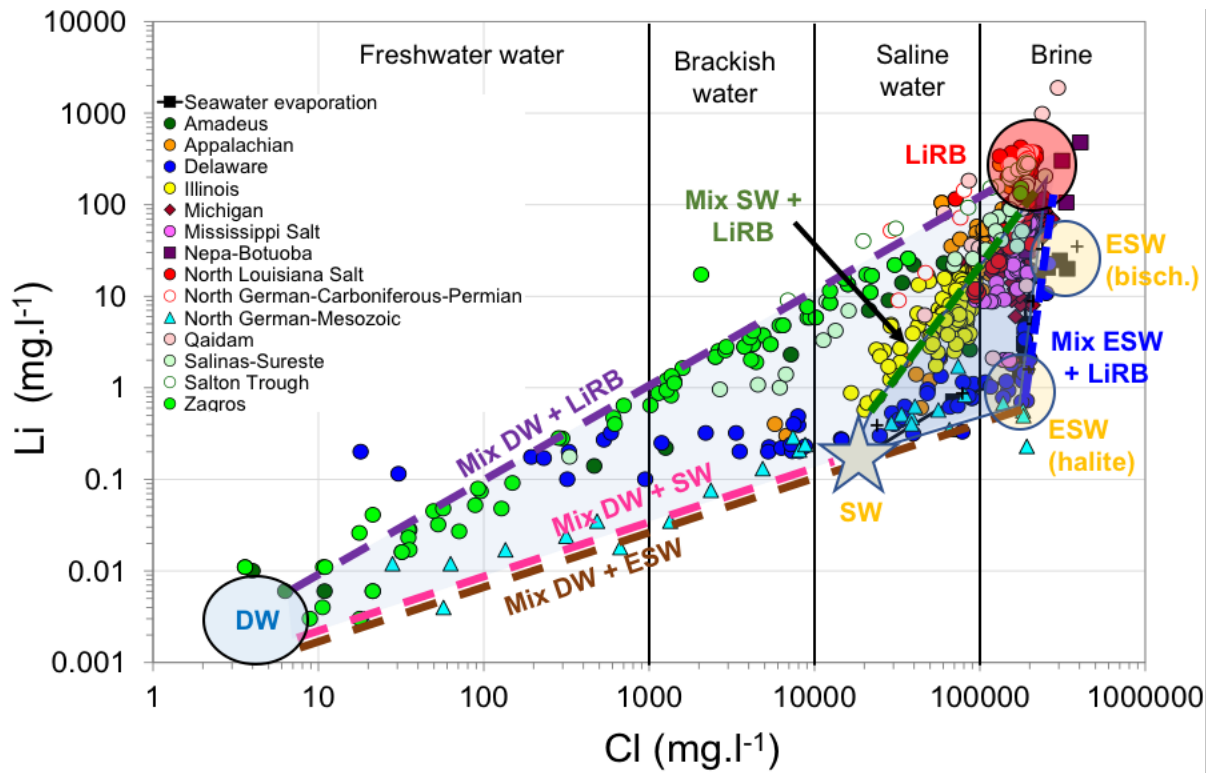


Fig. 4. Main trends of mixing of sedimentary formation waters. LiRB: Lithium rich brines, SW: seawater, DW: dilute water, ESW: evaporated seawater having passed halite saturation (halite) or bischofite saturation (bisch.) (after Fontes and Matray, 1993).

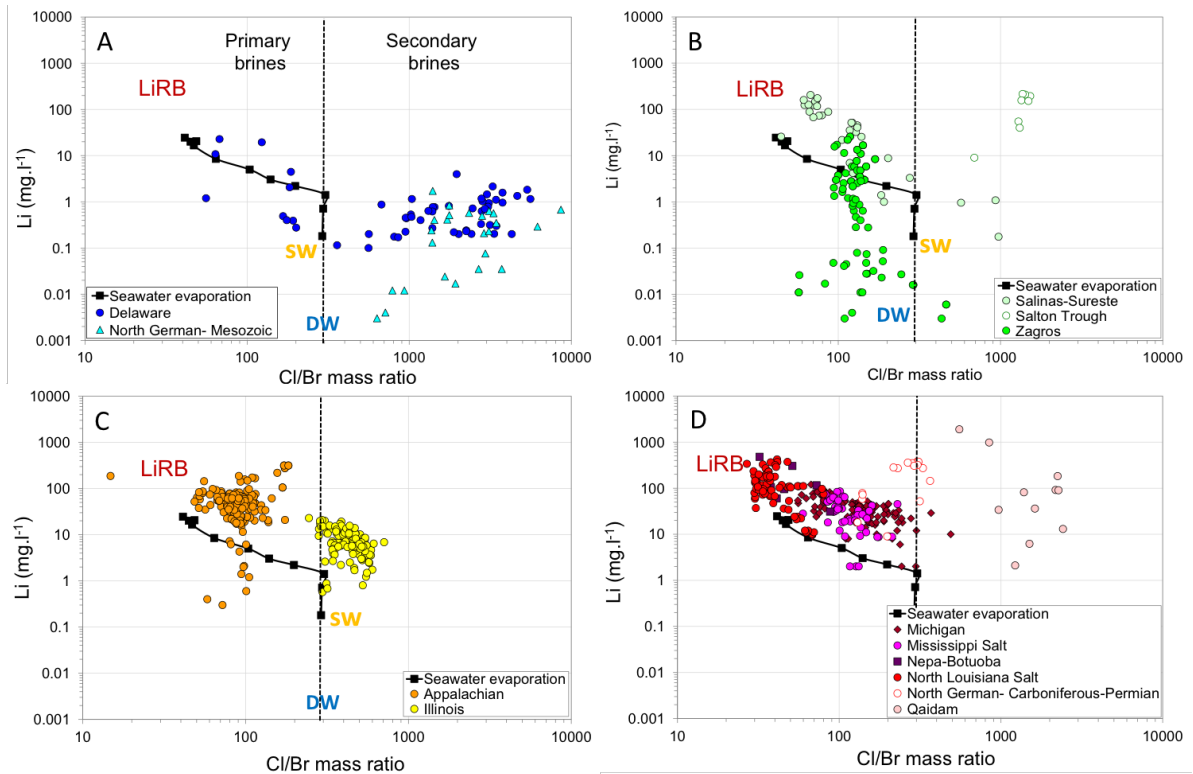


Fig. 5. Lithium concentration as a function of Cl/Br mass ratio in sedimentary formation waters. Data for basins with extended dilution trends are presented in A and B. The basins with high chlorinity close to the values of water saturated with respect to halite are in C and D. LiRB: Lithium rich brines, SW: seawater, DW: dilute water, seawater evaporation trend from Fontes and Matray (1993). Locations of DW and LiRB are indicative.

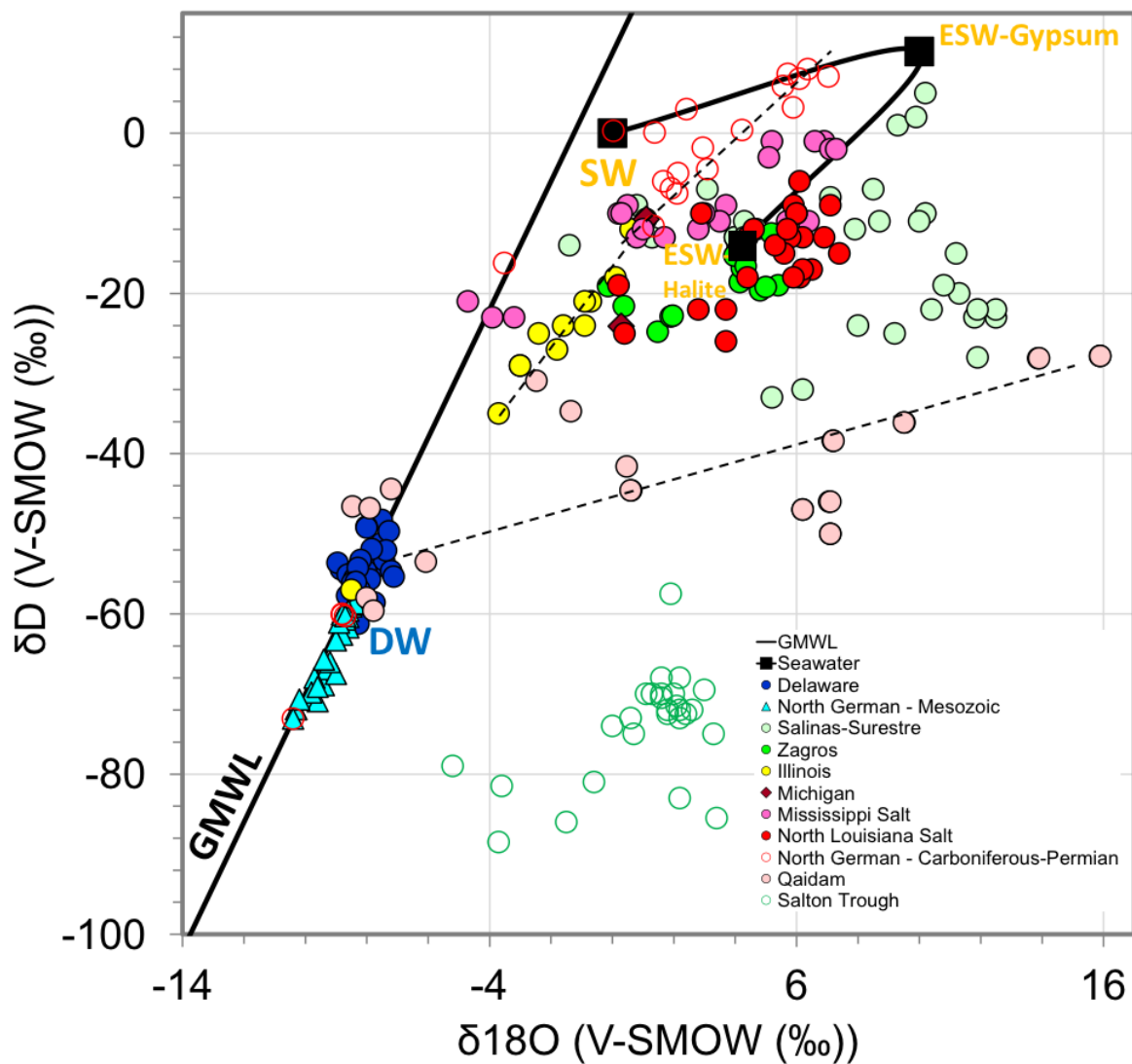


Fig. 6.  $\delta^{18}\text{O}$  as a function of  $\delta\text{D}$  (V-SMOW ‰). DW: dilute water, SW: seawater, ESW: evaporated seawater up to gypsum and halite, seawater evaporation trend (Knauth and Beeunas, 1986) and global meteoric water line (GMWL) (Craig, 1961). The blackdotted lines show the primary trend of mixing. References data: Delaware (Barnaby et al., 2004), Qaidam (Qichun et al., 2010. Tan et al., 2011), North German (Kloppman et al., 2001; Luders et al., 2010), Zagros (Bagheri et al., 2014a), Illinois (Stueber and Walter, 1991), Michigan (Wilson and Long, 1993a-b), Mississippi Salt (Kharaka et al., 1987), North Louisiana Salt (Moldovanyi and Walter, 1992), Salinas-Sureste (Birkle et al., 2009b) and Salton Trough (Williams and McKibben, 1989).

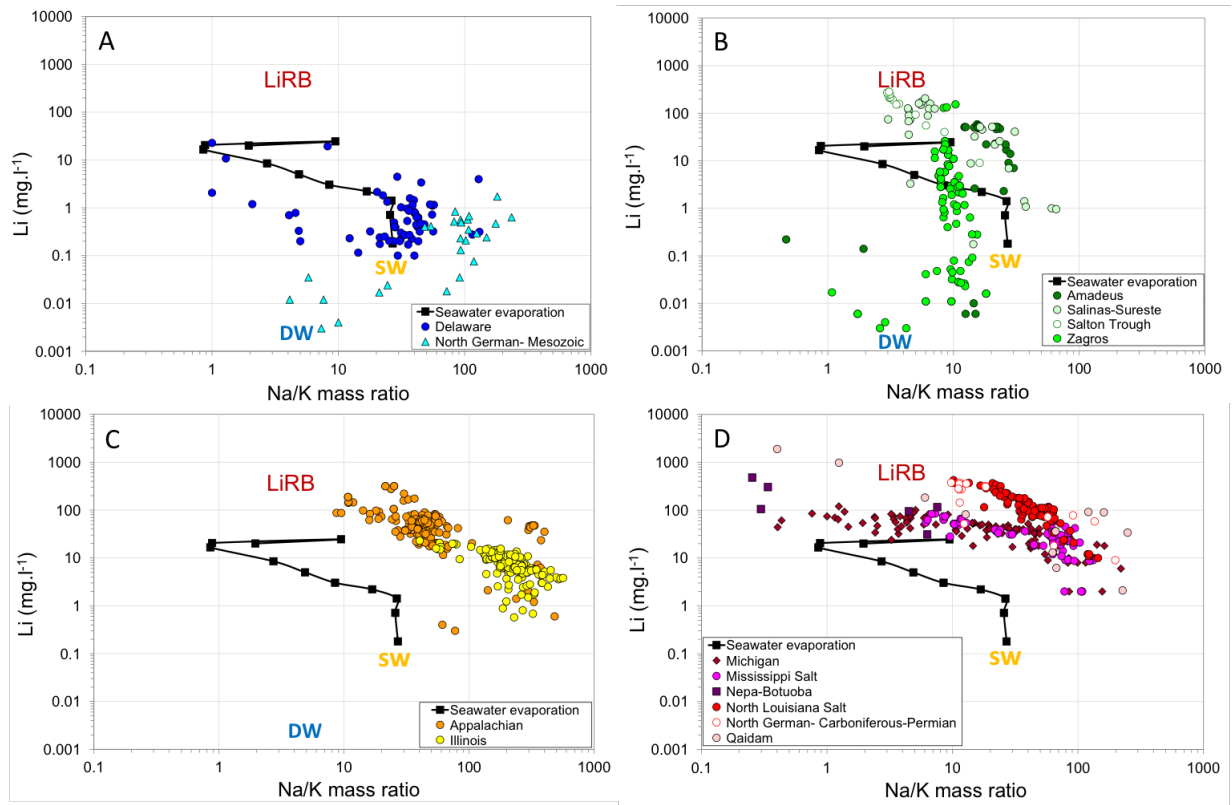


Fig. 7. Lithium concentration in sedimentary formation waters as a function of Na/K mass ratio. Data for basins with extended dilution trends of seawater are in A and B. The basins with high chlorinity close to the values of water saturated with respect to halite are in C and D. LiRB: Lithium rich brines, SW: seawater, DW: dilute water, seawater evaporation trend from Fontes and Matray (1993). Locations of DW and LiRB are indicative.

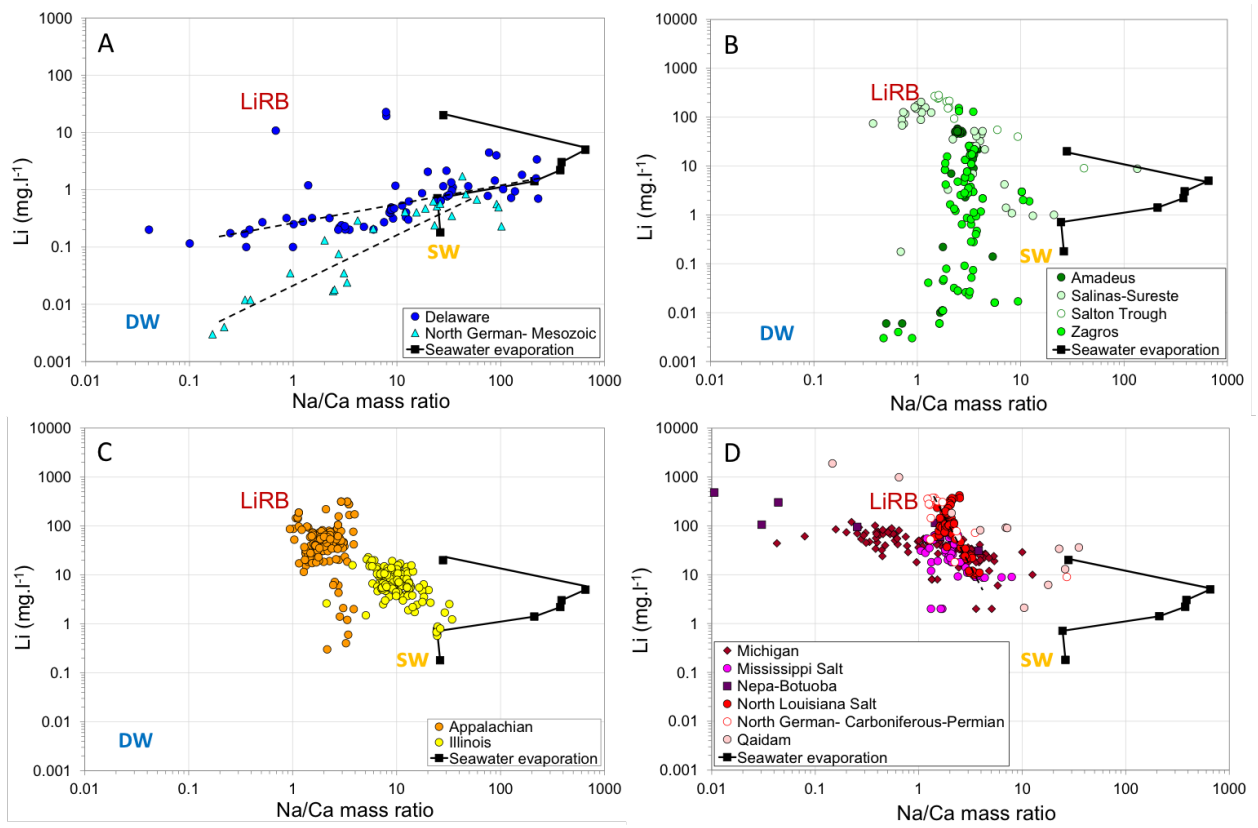


Fig. 8. Lithium concentration in sedimentary formation waters as a function of Na/Ca mass ratio. Data for basins with extended dilution trends are presented in A and B. The basins with high chlorinity close to the values of water saturated with respect to halite are in C and D. LiRB: Lithium rich brines, SW: seawater, DW: dilute water, seawater evaporation trend from Fontes and Matray (1993). Locations of DW and LiRB are indicative.

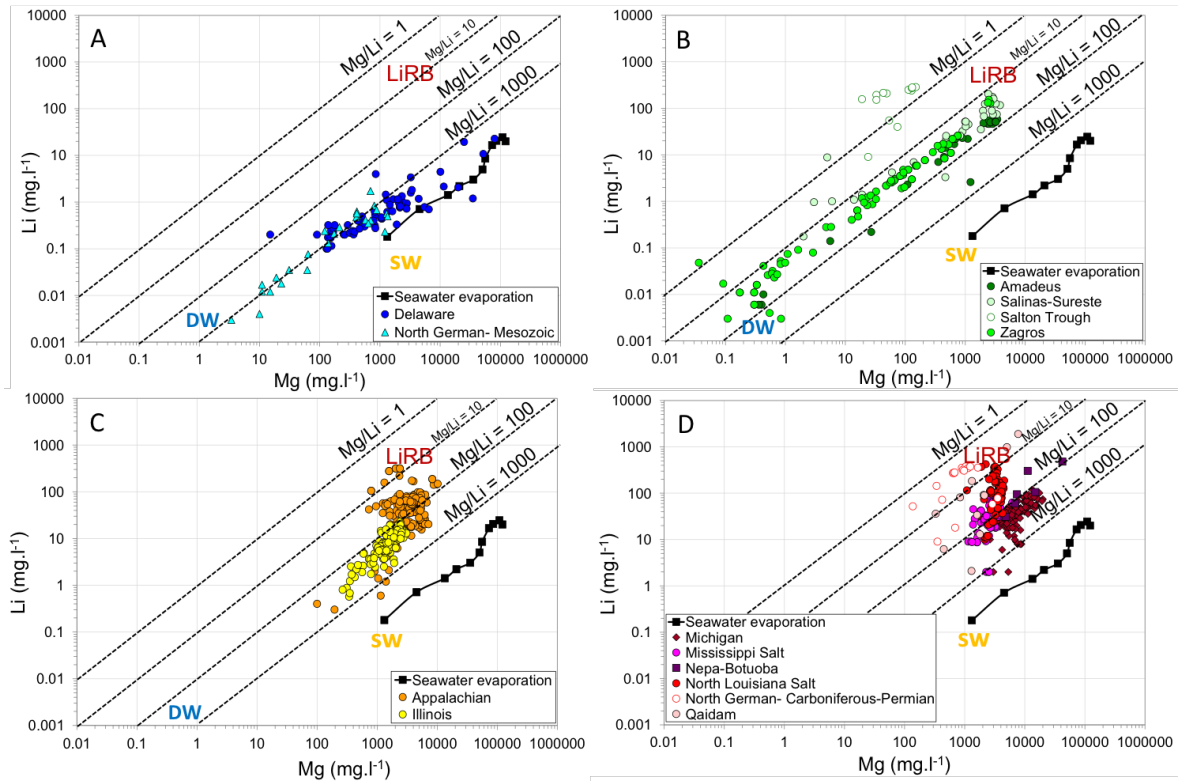


Fig. 9. Lithium concentration as a function of Mg concentration in sedimentary formation waters. Data for basins with extended dilution trends are presented in A and B. The basins with high chlorinity close to the values of water saturated with respect to halite are in C and D. LiRB: Lithium rich brines, SW: seawater, DW: dilute water, seawater evaporation trend from Fontes and Matray (1993). Locations of DW and LiRB are indicative.

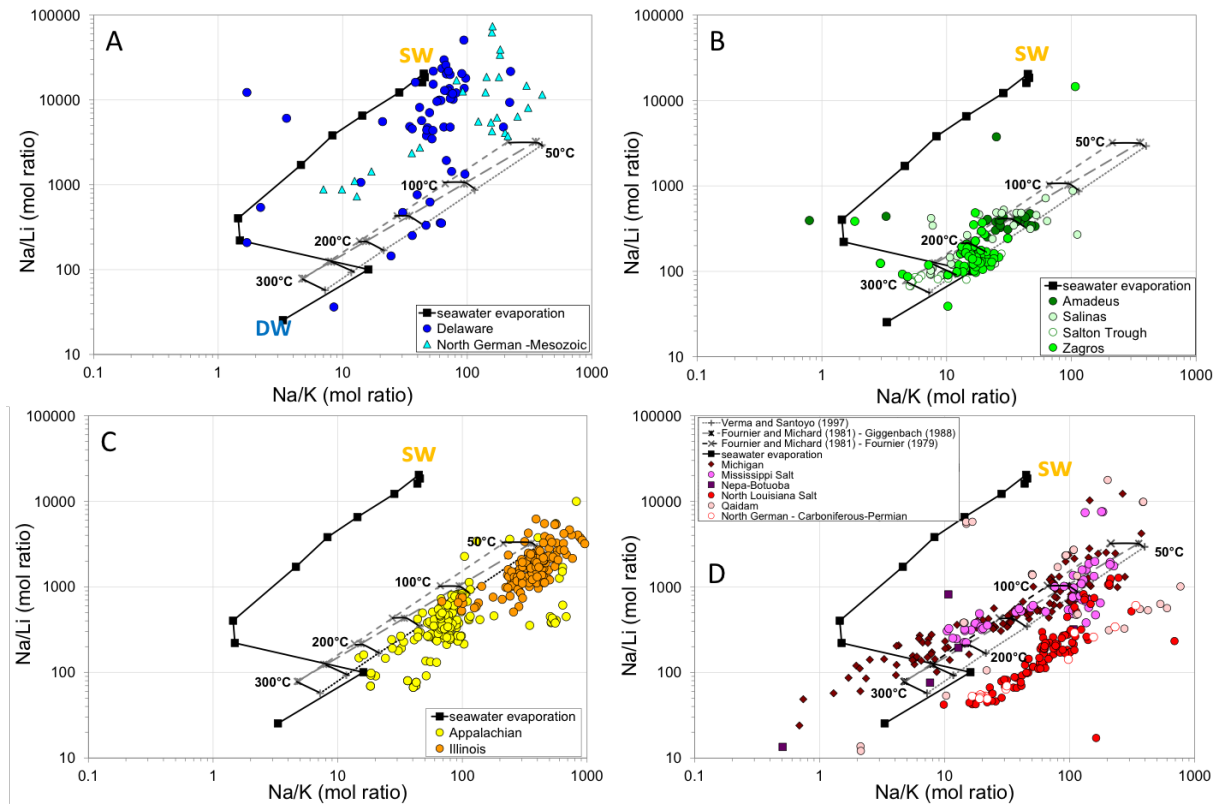


Fig. 10. Na/Li molar ratio in sedimentary formation waters as a function of Na/K molar ratio. Data for basins with extended dilution trends of seawater are in A and B. The basins with high chlorinities close to the values of water saturated with respect to halite are presented in C and D. SW: seawater, seawater evaporation trend from Fontes and Matray (1993). Dotted line: temperature estimation deduced from the geothermometric cation relationships (Fournier, 1979; Giggenbach, 1988; Fouillac and Michard, 1981; Verma and Santoyo, 1997).

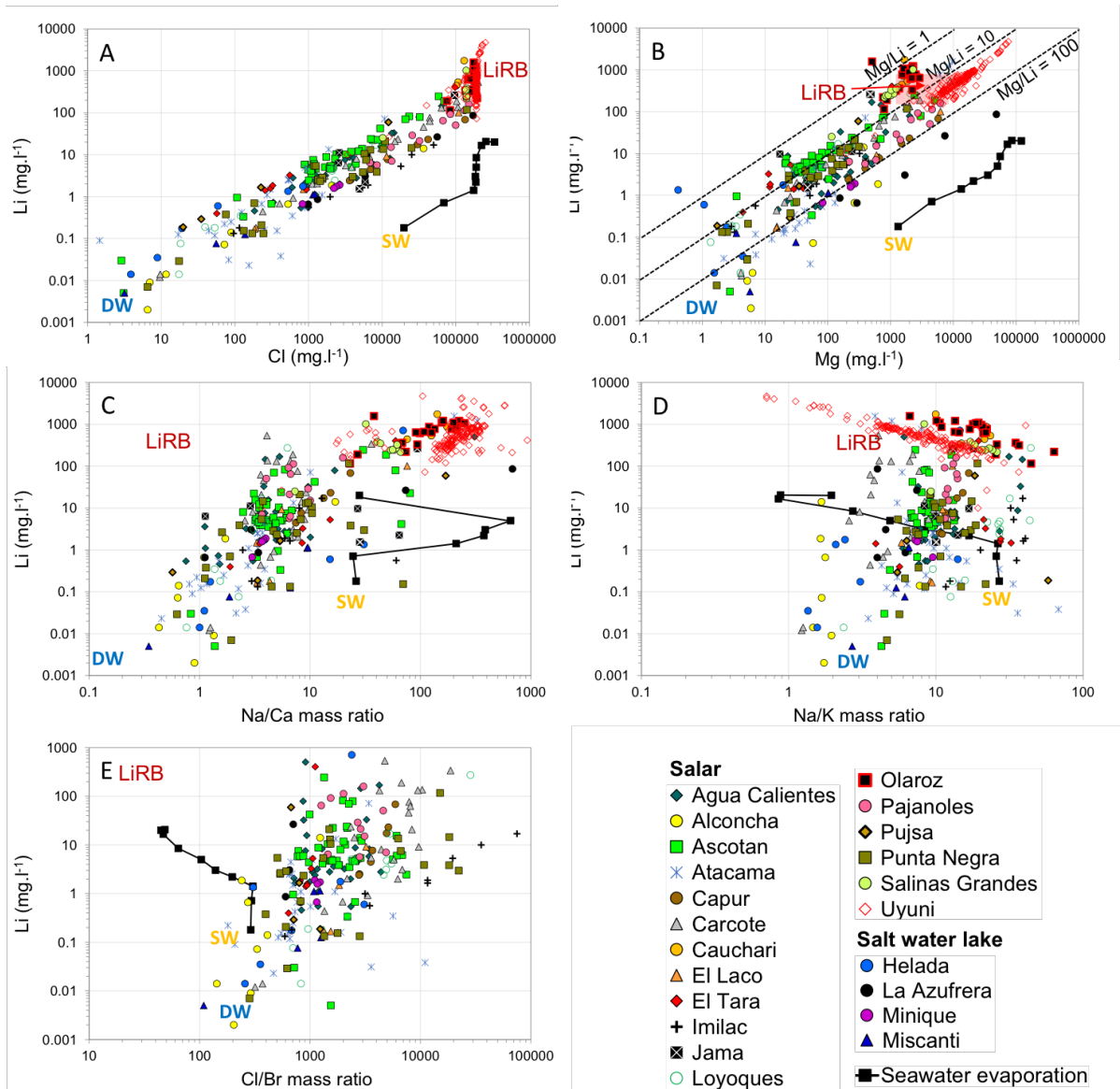


Fig. 11. Data from salars plotted in the chemical diagrams used for the sedimentary basin waters. Lithium concentration as a function of Cl concentration (A), Mg concentration with location of the LiRB brines in the pink inset indicated by the red arrow (B), Na/Ca (C) and Na/K (D) and Cl/Br (E) mass ratios. Main end-members SW: seawater, and end-members defined for sedimentary waters: LiRB: Li rich brines, and DW: dilute water are plotted for comparison. The seawater evaporation trend is reported from Fontes and Matray (1993). References data: Ericksen and Salas (1987), Risacher and Fritz (1991), Risacher et al. (1999), Lopez Steinmetz et al. (2018), Franco et al. (2020).

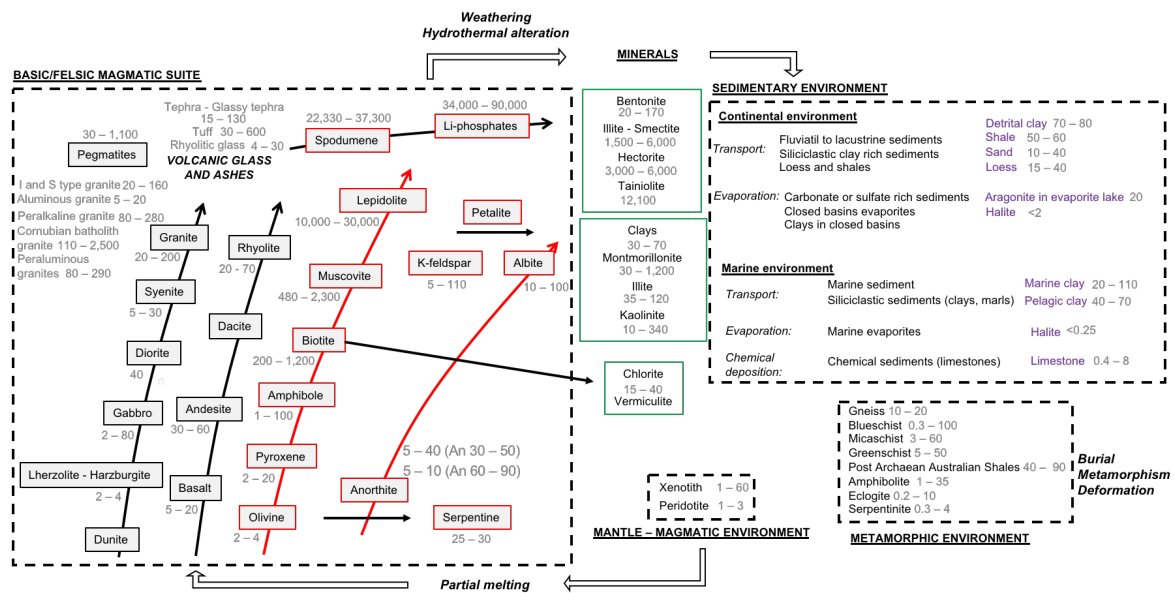
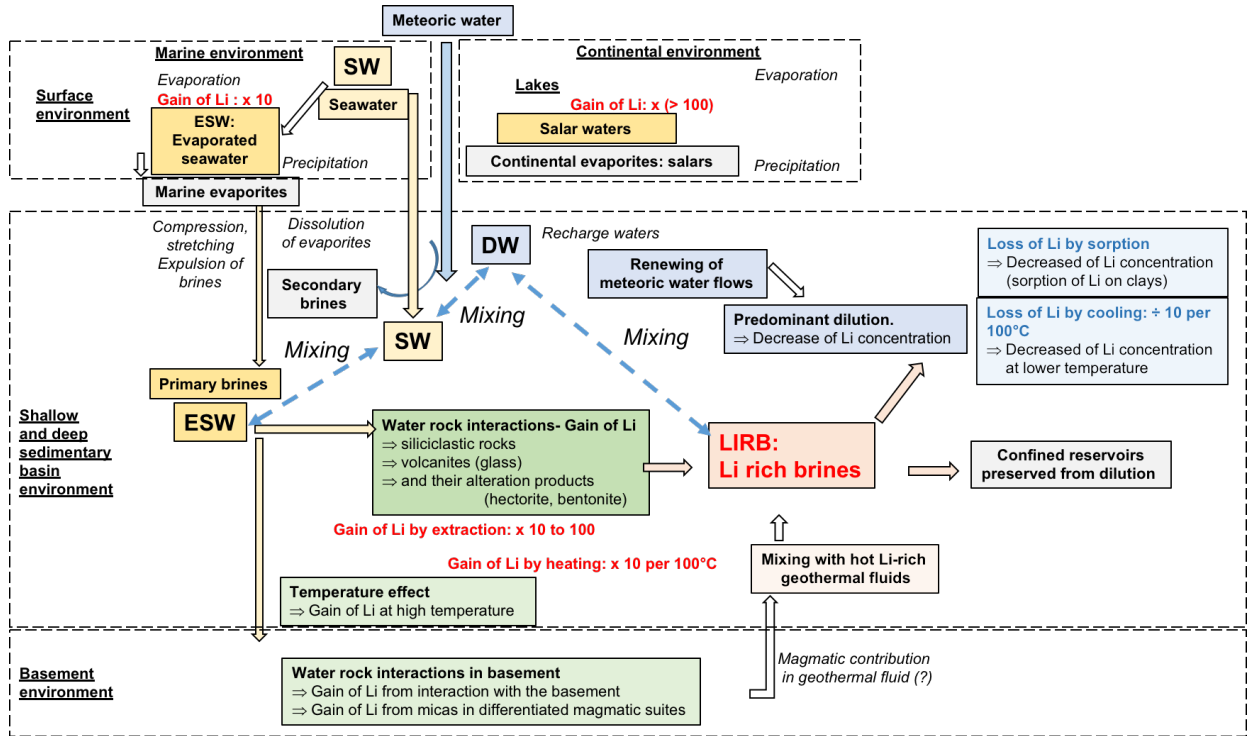


Fig. 12. Geochemical cycle and Li enrichment processes through rocks, minerals and sediments. In the left-hand side inset, the arrows indicate the main magma differentiation trends, with Li concentration range for main rock forming minerals. On the right-hand side, newly formed minerals during weathering and diagenesis, as well as the main sedimentary formations are listed. When possible, the main Li concentrations in rocks, minerals and sediments are indicated according to the 25<sup>th</sup> and 75<sup>th</sup> percentile of the data set of the lithium concentration values found in published sources. In a few cases, a single value appears when only one value is found in the literature. References are listed in the Supplementary references section (Supplementary references).

1



2  
3  
4

5 Fig. 13. Lithium through the crustal cycle. At the top of the diagram, the mechanisms of primary Li-  
 6 enrichment by evaporation from marine or continental waters yielding to marine evaporites on the  
 7 one hand and salars on the other hand; in the middle section, primary brines are expelled from  
 8 evaporites by squeezing of evaporites linked to compressional tectonics and salt tectonics, and  
 9 secondary brines formed by salt dissolution. They interact with sedimentary reservoir minerals or  
 10 layers bearing Li, and become Li-enriched. Interactions with basement rocks (bottom section) may  
 11 occur in some instances as well as Li inputs through hydrothermal waters. In blue the effect of recharge  
 12 waters in the dilution, cooling of the brines and the decrease of Li concentrations.

13

Table 1. Location of the selected sedimentary basins and chemical compositions (Li, Cl and Mg concentrations, Cl/Br, Na/Ca and Na/K ratios) of the formation waters. The minimum, maximum and mean values (in bracket) are given for set of waters.

Basin	Country	Age of sedimentary basin	Reservoir type	Li (mg.l <sup>-1</sup> )	Cl (mg.l <sup>-1</sup> )	Mg (mg.l <sup>-1</sup> )	Cl/Br mass ratio	Na/Ca mass ratio	Na/K mass ratio	References
Amadeus	Australia	Neoproterozoic - Devonian	Gas	0.006-60 (30)	4-189,960 (88,790)	0.4-3,430 (1,520)		0.5-5 (3)	0.5-30 (20)	Andrew et al., 2005
Nepa Botuoba (Siberian platform)	Russia	Neoproterozoic - Cambro-Ordovician	Oil and gas	31-480 (170)	184,900-405,700 (269,740)	3,700-42,200 (13,030)	30-90 (50)	0.01-4 (1)	0.3-60 (10)	Alexeev et al., 2020
Appalachian	USA	Silurian – Devonian	Oil and gas	0.3-320 (60)	5,760-247,000 (146,480)	100-10,200 (3,490)	15-180 (90)	1-4 (2)	9-480 (70)	Sanders, 1991 ; Skeen, 2010 ; Dresel and Rose, 2010
Illinois	USA	Silurian - Devonian	Oil and gas	0.6-20 (8)	16,630-97,220 (68,635)	270-3,080 (1,490)	240-710 (440)	2-30 (10)	40-560 (230)	Stueber and Walter, 1991 ; Stueber et al., 1993 ; Demir and Seyler, 1999
Michigan	USA	Silurian - Devonian	Oil	2-120 (40)	75,800-275,000 (186,950)	1,820-20,000 (7,960)	60-490 (140)	0.04-10 (2)	0.4-220 (40)	Wilson and Long 1993a - b
North German	Germany	Carboniferous - Permian	Gas	9-375 (220)	29,000-206,000 (145,130)	140-3,530 (1,070)	130-365 (255)	1-30 (3)	10-200 (40)	Lüders et al., 2010
Zagros	Iran	Paleo - Cenozoic	Oil and gas	0.003-30 (9)	4-177,500 (9,990)	0.04-2,630 (190)	60-460 (140)	0.2-50 (4)	1-55 (10)	Bagheri et al., 2014a-b
Delaware	USA	Permian - Triassic	Oil and gas	0.1-55 (2)	20-261,440 (68,800)	15-79,950 (4,870)	60-5,600 (1,890)	0.04-230 (30)	1-130 (35)	Bodine and Jones, 1990
North German	Germany	Mesozoic	-	0.003-2 (0.3)	630-8,625 (2,510)	3-1,340 (410)	20-192,000 (45,625)	0,20-100 (25)	4-235 (85)	Kloppmann et al., 2001
Mississippi Salt	USA	Jurassic - Miocene	Oil and gas	2-90 (35)	94,900-207,400 (164,050)	1,150-6,180 (2,640)	60-230 (120)	1-8 (2)	5-132 (50)	Carpenter et al., 1974; Kharaka et al., 1987
North Louisiana Salt	USA	Jurassic - Miocene	Oil	10-420 (130)	71,255-217,910 (168,340)	1,090-4,540 (3,340)	30-80 (40)	1-4 (2)	10-145 (50)	Moldovanyi and Walter, 1992
Salinas-Sureste	Mexico	Mesozoic - Cenozoic	Oil	0.2-205 (70)	330-248,000 (114,480)	2-3,810 (1,505)	45-970 (175)	0.4-135 (8)	3-70 (20)	Birkle et al., 2009a

Salton Trough	USA	Pleistocene - Holocene	Geothermal	9-280 (170)	6,900- 196,800 (122,000)	19-130 (70)	690-1,525 (1,305)	1-40 (6)	3-20 (5)	Thompson and Fournier, 1988; Williams and McKibben, 1989; Lippman et al., 1999
Qaidam	China	Late Tertiary - present-day	Oil	2-1,890 (260)	46,380- 297,000 (145,740)	330-7,780 (2,135)	550-2,420 (1,600)	0.1-35 (10)	0.4-250 (100)	Qishun et al., 2010; Tan et al., 2011

Basin names	Country	Age of sedimentary series	Presence of salt beds - diapirs	Description of the sedimentary series	Presence of volcanic and crystalline series	Reference
<b>Amadeus</b>	Australia	Late Proterozoic to Devonian	- Evaporites in Neoproterozoic and Cambrian formations, acting as seal	- Shallow marine to continental deposits - Shales and sandstones		Andrew et al., 2005 Jarrett et al., 2016 Mempes et al., 2020
<b>Siberian platform- Nepa Botuoba</b>	Russia	Neoproterozoic (Vendian) to Cambro-Ordovician	- Widespread Vendian (Lower Cambrian) salt bed - Salt-bearing formation deposited in a giant lagoon that covered the south half of the Siberian craton - Diapirism and salt anticline	- Salts are interbedded with strata of carbonaceous rocks (dolomites, limestones), and siliciclastic formations (sandstone, argillite)	- Archaean–Proterozoic crystalline basement, which is represented by quartzites, gneisses, schists and amphibolites - Devonian rift with volcanic rocks	Ulmishek, 2001
<b>Appalachian Michigan Illinois</b>	USA	Silurian to Devonian	Multiple beds, salt (halite, sylvite and carnallite with polyhalite, potash bearing unit, gypsum, anhydrite)	- Siltstone interbedded with silty shale and clayey shale - Salina group below the Marcellus shale (Mid Devonian oil source) and Oriskany sandstone reservoir - K-bentonite lenses below the Marcellus shale. - Brines in the Utica shale and limestones (Mid Ordovician) coming from the Beemantown group (anhydrite-halite)	Probable volcanic glass (?) transformed in K-bentonite (possible source rocks)	Blondes et al., 2020 Mount, 2014 Rine, 2015 Smith, 2013
<b>Zagros</b>	Iran	Four significant phases: - early Paleozoic intra-cratonic pull-apart basin and platform margin basin, - late Paleozoic platform margin basin, - Mesozoic passive continental margin basin, - Cenozoic foreland basin (Eocene to Pleistocene)	- Proterozoic to Early Cambrian Hormuz salt layer with a thick and continuous salt layer - Evaporite and mudstone of the Gasharan formation (early Miocene): main seals in the foredeep zone - Gasharan evaporite (Fars salt) resulting in part of the dissolution-redeposition of the Hormuz salt - Upper Eocene salt layers with anhydrite, halite and sylvite	- Deep marine hemipelagic – pelagic calcareous shale, marl and limestone with subordinate argillaceous limestone.  - Reservoirs in the foredeep zone. Paleozoic reservoir with Silurian, source rock and Meso-Cenozoic reservoirs with Lower Cretaceous source rock.		Liu et al., 2018 Jahani et al., 2009
<b>Delaware</b>	USA	Permian to Triassic	Multiple beds (halite, anhydrite)	- Sand and sandstone - Siltstone and sandstone - Mudstone and siltstone		Engle et al., 2016
<b>North German</b>	Germany	Three significant phases: - rifting initiated during the late Carboniferous, followed by 20 Ma subsidence period (Rotliegend sediments).	- Top of Rotliegend-Zechstein is made of carbonates and evaporate deposits. - Keuper includes dolomite, shale and evaporites. - Several reservoir rocks are	- Siliciclastic series shale, lacustrine evaporites, carbonate, sulphate, salts. - Petroleum system includes Carboniferous and Permian Rotliegend formations	- Abundant volcanic successions of Permian age above a carboniferous basin - Igneous intrusions (diabase dikes)	Luders et al., 2010

		<ul style="list-style-type: none"> <li>- rifting during Triassic followed by subsidence and sediment deposition.</li> <li>- rifting during late Jurassic in response to the North Sea coming event</li> </ul>	<p>observed below and above the massive Trias salt formation.</p> <ul style="list-style-type: none"> <li>- Salt tectonic as diapirism</li> </ul>			
<b>Gulf Coast: Mississippi Salt North Louisiana Salt</b>	USA	<ul style="list-style-type: none"> <li>- Jurassic to Miocene</li> </ul>	<ul style="list-style-type: none"> <li>- Salt tectonics (diapirs) linked to the behaviour of the Mid Jurassic Louann evaporite formation</li> <li>- Louann formation includes halite salt layers (coarsely recrystallised) with streak of anhydrite</li> <li>- Buckner anhydrite formation</li> </ul>	<ul style="list-style-type: none"> <li>- Deltaic, non-marine and continental sandstone and shale.</li> <li>- Carbonate series (laminated lime and dolomitic limestone)</li> <li>- Norplet fluvial and aeolian siliciclastic formation above the Louann salt formation and the Smackover formation</li> </ul>	<ul style="list-style-type: none"> <li>- Local igneous intrusions (diabase dikes) but not acting as evident Li- source</li> </ul>	<p>Carpenter et al., 1974 Land et al., 1988 Rogers et al., 2006 Zhang et al., 2013 Hudec et al., 2013a-b</p>
<b>Salinas- Sureste basin</b>	Mexico	<ul style="list-style-type: none"> <li>- Mesozoic series (from Kimmeridgian to late Cretaceous) to Cenozoic series.</li> </ul>	<ul style="list-style-type: none"> <li>- Salt layers linked to the opening of the Mexico Gulf (Callovia)</li> <li>- Salt tectonics and diapirs forming isolated shallow salt bodies</li> <li>- Strong Miocene diapirism</li> <li>- Anhydrite layer</li> </ul>	<ul style="list-style-type: none"> <li>- Carbonate formations (dolomite, limestone) and mudstones</li> <li>- Shallow oil reservoirs linked to salt tectonics</li> </ul>		<p>Birkle et al., 2009 a-b Comision de hidrocarburos, 2015</p>
<b>Qaidam</b>	China	<ul style="list-style-type: none"> <li>- Late Cenozoic (Pliocene) to present-day</li> </ul>	<ul style="list-style-type: none"> <li>- Evaporite layers corresponding to lacustrine water evaporation</li> <li>- Two periods of salt formation in the Qaidam basin: Late Tertiary Pliocene and Late Quaternary Pleistocene</li> </ul>	<ul style="list-style-type: none"> <li>- Lacustrine sediments: limestone, sandstone, shale, mudstone with anhydrite, halite beds sandstones</li> <li>- Three lakes evolved into salt lakes in the second salt-forming period</li> </ul>		<p>Zhang, 1987 Ma et al., 2021 Cheng et al., 2018</p>
<b>Salton Though</b>	USA	<ul style="list-style-type: none"> <li>- Pleistocene to Holocene</li> </ul>	<ul style="list-style-type: none"> <li>- Evaporite</li> </ul>	<ul style="list-style-type: none"> <li>- Fluvial, deltaic, lacustrine, evaporite</li> <li>- Low-density siliciclastic sediments and sedimentary rocks from Holocene to Pleistocene</li> <li>- Overlying pre-Salton Trough continental crust</li> <li>- Hydrothermal metamorphism producing greenschist and amphibolite facies hornfelses</li> </ul>	<ul style="list-style-type: none"> <li>- Locally intruded by both mafic and felsic igneous rocks</li> <li>- Pre-Salton Trough continental crust consists of Mesozoic granitoids, intrusive in Precambrian gneiss and schists and Miocene volcanic rocks</li> </ul>	<p>Hulen et al., 2002</p>

Table 2. Geological characteristics of the sedimentary basins used in this study, listed as a function of their age from the Proterozoic to the Quaternary.

Basin name	Basin type	Region	Country	Li (mg.l <sup>-1</sup> )	Cl (mg.l <sup>-1</sup> )	Mg (mg.l <sup>-1</sup> )	Cl/Br mass ratio	Na/Ca mass ratio	Na/K mass ratio	References
Agua Calientes (1,2,3,4)	Salar	Puna de Atacama	Chile	0.5-500	190-175000	20-12300	720-4400	1-300	6-40	Risacher et al., 1999
Alconcha		Puna de Atacama	Chile	0.002-15	6-36600	2-630	130-1250	0.5-20	1-10	Risacher et al., 1999
Ascotan		Puna de Atacama	Chile	0.005-250	3-70000	3-5130	700-7500	1-80	4-10	Risacher et al., 1999
Atacama		Puna de Atacama	Chile	0.02-1570	2-189500	2-9650	180-11030	0.5-330	3-70	Ericksen and Salas 1987 Risacher et al., 1999
Capur		Puna de Atacama	Chile	2-70	3620-134000	210-5800	2780-5930	7-20	10-20	Risacher et al., 1999
Carcote		Puna de Atacama	Chile	0.01-540	10-202000	4-9000	320-18750	1-40	2-20	Risacher et al., 1999
Cauchari		Puna	Argentina	440-1740	102200-163900	1510-2100		80-210	10-20	Steinmetz et al., 2018
El Laco		Puna	Chile	0.2-100	190-109630	15-6250	1320-3220	3-80	6-15	Ericksen and Salas 1987 Risacher et al., 1999
El Tara		Puna	Chile	0.5-400	60-98000	4-1050	640-1110	2-60	4-30	Risacher et al., 1999
Imilac		Puna de Atacama	Chile	0.1-20	100-50100	3-600	590-74900	2-60	10-40	Risacher et al., 1999
Jama		Puna	Argentina	2-260	2560-97020	20-500		1-90	8-20	Steinmetz et al., 2018
Loyoques		Puna	Chile	0.01-270	17-148000	1-2070	700-28400	1-6	2-40	Risacher et al., 1999
Olaroz		Puna	Argentina	115-1570	76000-196000	510-2900		20-250	7-60	Steinmetz et al., 2018 Franco et al., 2020
Pajonales		Puna de Atacama	Chile	6-160	6850-151000	220-6200	1260-4890	4-20	10-15	Risacher et al., 1999
Pujsa		Puna de Atacama	Chile	0.2-60	20-12200	2-310	670-1240	1-170	5-60	Risacher et al., 1999
Punta Negra		Puna de Atacama	Chile	0.01-120	7-142000	0.1-1830	280-22230	0.6-70	5-20	Risacher et al., 1999
Salinas Grandes		Puna	Argentina	25-1020	10200-141350	115-2300		7-70	8-30	Steinmetz et al., 2018
Uyuni	Altiplano	Bolivia	10-4720	3400-253000	200-75300		4-930	1-40	Risacher and Fritz 1991	
Helada	Salt water lake	Puna de Atacama	Chile	0.01-710	4-179000	0.4-2450	260-3100	1-70	1-15	Risacher et al., 1999
La Azufrera		Puna de Atacama	Chile	1-90	1000-172130	160-48640	600-820	1-680	4-7	Ericksen and Salas 1987 Risacher et al., 1999
Minique		Puna de Atacama	Chile	1-2	830-2650	80-270	1100-1230	3-4	7-9	Risacher et al., 1999
Miscanti		Puna de Atacama	Chile	0.005-1	3-1210	4-100	110-1260	0.3-10	3-7	Risacher et al., 1999

Table 3. Location of the selected closed basins from South America and related water chemical compositions (Li, Cl and Mg concentrations, Cl/Br, Na/Ca and Na/K ratios). The minimum and maximum values are given for each set of analysed waters.

